AWARD NUMBER: W81XWH-13-1-0210

TITLE: Citrullinated Chemokines in Rheumatoid Arthritis

PRINCIPAL INVESTIGATOR: David A. Fox

CONTRACTING ORGANIZATION: Regents of the University of Michigan

Ann Arbor, MI 48109-1274

REPORT DATE: October 2015

TYPE OF REPORT: Annual

PREPARED FOR: U.S. Army Medical Research and Materiel Command
Fort Detrick, Maryland 21702-5012

DISTRIBUTION STATEMENT: Approved for Public Release;
Distribution Unlimited

REPORT DOCUMENTATION PAGE

Form Approved
OMB No. 0704-0188

1. REPORT DATE October 2015	2. REPORT TYPE Annual	3. DATES COVERED 30 Sep 2014 - 29 Sep 2015

4. TITLE AND SUBTITLE

Citrullinated Chemokines in Rheumatoid Arthritis

5a. CONTRACT NUMBER

5b. GRANT NUMBER
W81XWH-13-1-0210

5c. PROGRAM ELEMENT NUMBER

6. AUTHOR(S)
David A. Fox, MD

E-Mail: dfox@umich.edu

5d. PROJECT NUMBER

5e. TASK NUMBER

5f. WORK UNIT NUMBER

7. PERFORMING ORGANIZATION NAME(S) AND ADDRESS(ES)

Regents of The University Of Michigan
503 Thompson St.
Ann Arbor, MI 48109-1340

8. PERFORMING ORGANIZATION REPORT NUMBER

9. SPONSORING / MONITORING AGENCY NAME(S) AND ADDRESS(ES)

U.S. Army Medical Research and Materiel Command
Fort Detrick, Maryland 21702-5012

10. SPONSOR/MONITOR'S ACRONYM(S)

11. SPONSOR/MONITOR'S REPORT NUMBER(S)

12. DISTRIBUTION / AVAILABILITY STATEMENT

Approved for Public Release; Distribution Unlimited

13. SUPPLEMENTARY NOTES

14. ABSTRACT

Citrullination, catalysed by peptidylarginine deiminase (PAD), is a post-translational modification of arginine to citrulline, which contributes to the pathogenesis of rheumatoid arthritis (RA). We show that citrullinated epithelial-derived neutrophil-activating peptide 78/CXCL5 (cit-ENA-78/CXCL5) is significantly higher in RA synovial fluids (SFs) compared to osteoarthritis (OA) and other inflammatory rheumatic diseases (OD) SFs, and its concentration correlates with RA disease activity. Citrullinated chemokine concentrations were measured by enzyme linked immunosorbent assay (ELISA) in RA and normal (NL) sera and in RA, osteoarthritis (OA), and other inflammatory rheumatic disease (OD) synovial fluids (SFs). The correlation between the citrullinated chemokine levels and clinical data was analyzed. A strong correlation was found between the amounts of citENA-78/CXCL5 and C-reactive protein or erythrocyte sedimentation rate (ESR) in RA SFs. These results indicate that citENA-78/CXCL5 may have novel inflammatory properties in RA pathogenesis.

15. SUBJECT TERMS
Citrullination, chemokines, chemotaxis, rheumatoid arthritis, immunology

16. SECURITY CLASSIFICATION OF: U			17. LIMITATION OF ABSTRACT	18. NUMBER OF PAGES	19a. NAME OF RESPONSIBLE PERSON USAMRMC
a. REPORT U	b. ABSTRACT U	c. THIS PAGE U	UU		19b. TELEPHONE NUMBER *(include area code)*

Standard Form 298 (Rev. 8-98)
Prescribed by ANSI Std. Z39.18

Table of Contents

1. Introduction

Citrullination, catalysed by peptidyl arginine deiminase (PAD) enzymes, is a post-translational modification of arginine to citrulline that contributes to the pathogenesis of rheumatoid arthritis (RA). Chemokines, which play an important role in the development of RA, can be citrullinated *in vitro*. We are examining whether citrullinated chemokines are detected in RA biological fluids, and if so, what their biological activities are. We posit that modification of seminal chemokines in the RA synovial fluid (SF) confers unique properties that significantly modify the inflammatory environment of the RA joint. Chemokines, including epithelial-derived neutrophil-activating peptide 78 (ENA-78/CXCL5), play a critical role in the development of RA, and are involved in inflammatory leukocyte migration into rheumatoid synovial tissue (ST). Recent studies have shown that several chemokines, ENA-78/CXCL5, interleukin-8 (IL-8/CXCL8), interferon gamma-induced protein 10 (IP-10/CXCL10), interferon-inducible T-cell alpha chemoattractant (I-TAC/CXCL11), and stromal derived factor-1α (SDF-1α/CXCL12), can be citrullinated by PAD *in vitro*. We also found that a regulatory nuclear protein, inhibitor of DNA binding-1 protein (Id1) can regulate fibroblast chemokine expression and can also be found in citrullinated form in RA tissues. In this study, we want to investigate whether ENA-78/CXCL5, macrophage inflammatory protein-1α (MIP-1α/CCL3), and monocyte chemotactic protein-1 (MCP-1/CCL2), which are representative chemokines in RA, are citrullinated in RA, osteoarthritis (OA), and normal (NL) control subjects. We then want to examine the properties of these modified chemokines to explore their novel functions that will offer additional insight into the function of chemokines in chronic diseases such as RA.

2. Keywords

Rheumatoid arthritis (RA)
Osteoarthritis (OA)
Normal (NL)
Synovial Fluid (SF)
Synovial Tissue (ST)
Serum
Chemokines
Chemotaxis
Anti-cyclic-citrullinated peptide antibodies (anti-CCP or ACPA)
Liquid chromatography coupled with tandem mass spectrometry (LC-MS/MS)
Citrullination
Enzyme Linked Immunosorbant Assay (ELISA)
Epithelial Neutrophil Chemoattractant Peptide-78 (ENA-78/CXCL5)
Monocyte Chemoattractant Protein-1 (MCP-1/CCL2)
Macrophage Inflammatory Protein-1 alpha (MIP-1α/CCL3)
Peptidyl Arginine Deiminase (PAD)
Neutrophils (PMNs)
Monocytes
Arginine
Post-translational
Inhibitor of DNA binding-1 (Id1)

3. Overall Project Summary

Current Objectives: **Specific Aim 1: To determine how citrullinated chemokines compare in RA, vs. OA, vs. other rheumatic diseases (OD), vs. NLs.**

Major Task 1: Characterize citrullinated chemokines in RA.

Subtask 1: SF and sera will be obtained from patients with RA, OA or ODs and assayed for key citrullinated and non-citrullinated chemokines thought to be important in the pathogenesis of RA. Subtask 2: ST will be obtained from RA, OA, or NL joints, homogenized and assayed for citrullinated and non-citrullinated chemokines.

Summary of Results: We have been actively recruiting patients for this study. We currently have enough patient fluids and tissues to perform all assays proposed in this grant. We have generated data to show that ENA-78/CXCL5, MIP-1α/CCL3 and MCP-1/CCL2 can all be detected in RA SFs. We have made tissue homogenates obtained from patients with RA and OA, and from NL ST obtained from tissue repositories. Using these homogenates, we have shown that RA ST joint homogenates contain citrullinated (cit) ENA-78/CXCL5 and that this can be detected by Western blotting analysis.

Progress and Accomplishments: Citrullination is a post-translational modification mediated by PAD. Chemokines, which play an important role in the development of RA, can be citrullinated *in vitro*. We undertook this study to examine whether the citrullinated chemokines ENA-78/CXCL5, MIP-1α/CCL3, and MCP-1/CCL2 are detected in RA biological fluids, and if so, what their biological activities are. Recombinant human (rh) chemokines were citrullinated by PAD. Citrullinated chemokine concentrations were measured by enzyme linked immunosorbent assay in RA and normal sera and in RA, OA, and OD SFs. The correlation between the citrullinated chemokine levels and clinical data was analyzed. We found that citENA-78/CXCL5 was significantly higher in RA sera and SFs than normal sera and OD including OA SFs, respectively (figure 1). A strong correlation was found between the amount of citENA-78/CXCL5 and C-reactive protein or erythrocyte sedimentation rate in RA SFs. Our conclusions for the first year of experiments is that citENA-78/CXCL5 can be detected in RA tissues and is highly correlated with RA disease activity.

Taken together, evidence is strong for citrullination being integral to inflammation and the pathogenesis of RA. Inflammatory cytokines are known to be perpetuators of the disease process, but they may also be more than that. If our hypothesis is correct, citrullinated chemokines may be present and

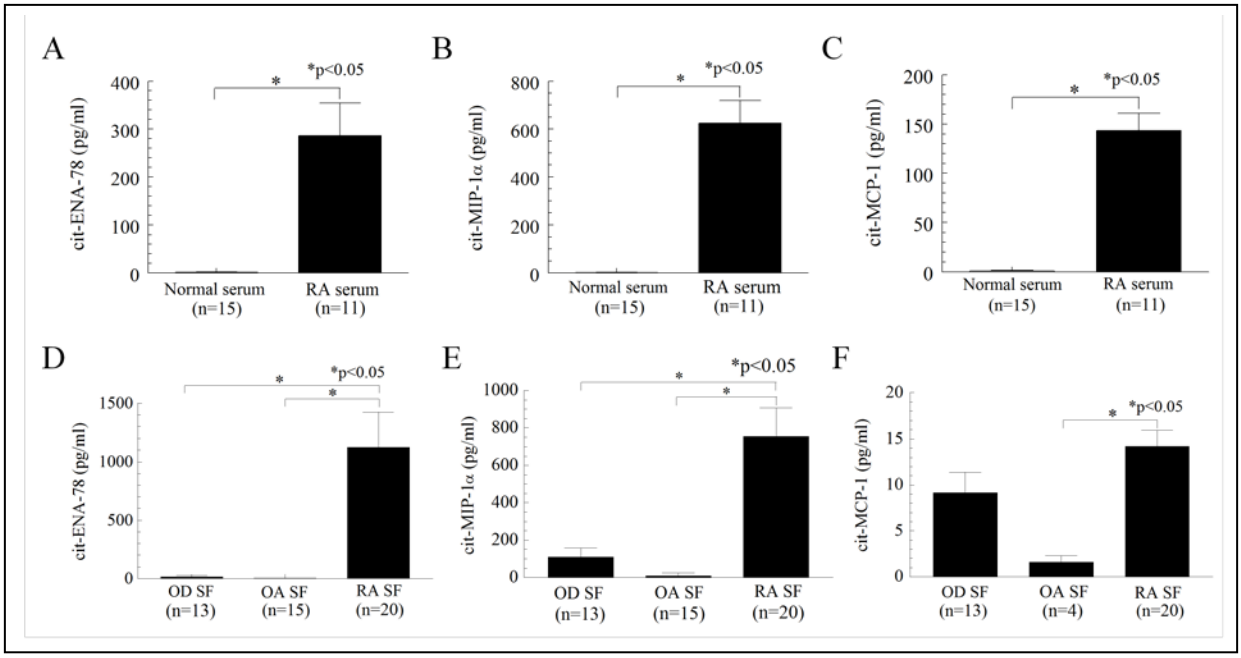

Figure 1.Citrullinated chemokines are highly expressed in RA sera and SFs. Citrullinated chemokines were measured using an ELISA in which chemokines were captured on an ELISA plate followed by detection with anti-modified citrulline after chemical modification of citrulline residues. RF (rheumatoid factor) was depleted from RA SFs and sera prior to the ELISA assay. A), B), and C), CitENA-78/CXCL5, MIP-1α/CCL3, and MCP-1/CCL2 concentrations in RA and normal sera. These citrullinated chemokines were all greater in RA compared to normal sera. D), E), and F) CitENA-78/CXCL5, MIP-1α/CCL3, and MCP-1/CCL2 concentrations in RA, OD, and OA SFs. CitENA-78/CXCL5 and MIP-1α/CCL3 were significantly greater in RA SFs than in OA and OD SFs. CitMCP-1/CCL2 was higher in RA compared to OA SFs. Bars show the mean ± SEM (n = the number of patients). *p<0.05 was considered significant. cit-ENA-78 = citrullinated ENA-78/CXCL5; cit-MIP-1α = citrullinated MIP-1α/CCL3; cit-MCP-1 = citrullinated MCP-1/CCL2.

pathogenic early in the course of RA. These preliminary studies should establish whether this is the case for key chemokines involved in RA pathogenesis. The results of these studies will also help us determine if citrullinated chemokines should be pursued as potential biomarkers for RA. We have recently published a manuscript supporting our hypothesis[1], and have shown that citrullination can effect chemokine activity and be associated with markers of disease severity.

Current Objectives: **Specific Aim 2: To determine the mechanisms of citrullination of chemokines leading to altered chemokine function in RA.**

Major task II: To determine the cellular signaling pathways induced by citrullinated chemokines.

Subtask 1: Leukocyte chemotaxis assays, modifying chemokines containing ELR motif and mass spec analysis, site directed mutagenesis of chemokines.

Subtask 2: Signal transduction analysis of endothelial cells and leukocytes.

Summary of Results: LC-MS/MS analysis confirmed citrullination of citENA78/CXCL5. CitENA78/CXCL5-induced monocyte (MN) migration was significantly reduced by Jnk and NFκB inhibitors, but not by inhibitors of Src, p38, and Erk1/2. We found that Jnk siRNA-transfected MNs displayed decreased citENA78/CXCL5-induced MN migration compared to control transfected MNs and that citR45K and citR48K mutations significantly reduced MN chemotaxis, suggesting that citENA78/CXCL5-induced MN migration is dependent, at least partially, on both citrulline residues (figure 2). We also tested these findings in vivo using the air pouch model. The mouse air pouch model showed marked MN recruitment in response to citENA78/CXCL5 compared to the controls, suggesting that citENA78/CXCL5 increases MN ingress in vivo. CitENA78/CXCL5-stimulated MNs showed increased expression of phosphorylated-Jnk and phosphorylated-NFκB (p-NFκB) which was inhibited by signaling inhibitors. We discovered that a Jnk inhibitor reduced the level of p-NFκB, suggesting that Jnk is upstream of NFκB in citENA78/CXCL5-stimulated MNs. We also found that citENA78/CXCL5 induces MN migration via Jnk and NFκB signaling pathways. Therefore, we could conclude that MN chemotaxis induced by citENA78/CXCL5 is partially dependent on both citrulline residues.

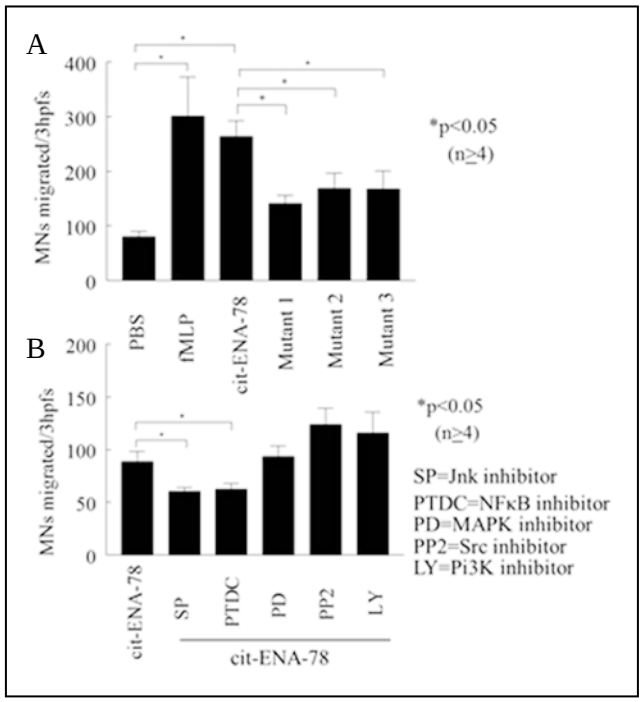

Figure 2. *MN chemotaxis and signaling inhibition to citENA-78/CXCL5*: MN migration assays were performed by placing cells in a 48-well Neuroprobe microchemotaxis chamber. As shown, MNs are chemotactic for citENA-78/CXCL5. A. To determine the mechanism involved, MN chemotaxis assay was performed with citENA78/CXCL5 in modified Boyden chambers to mutants (R45K, R48K and R45/48K) of rhENA-78/CXCL5. Mutants were generated by transmutation of arginines to lysines and were used in MN chemotaxis assays. CitR45K and citR48K mutations significantly reduced MN chemotaxis, suggesting that citENA78/CXCL5-induced MN migration is dependent, at least partially, on both citrulline residues. B. To determine the kinases required for citENA-78 mediated MN chemotaxis to citENA-78/CXCL5, cells were incubated with chemical signaling inhibitors. MNs were preincubated with chemical signaling inhibitors for 1 h prior to the assay, and the inhibitors were present in the upper chamber with the MNs during the assay. The following inhibitors were purchased from and used at concentrations recommended by Calbiochem (La Jolla, CA): PD98059 (10μM Erk1/2 inhibitor), PDTC (100μM NFκB inhibitor), LY294002 (10μM PI_3K inhibitor), SP (Jnk inhibitor) and PP2 (1μM Src inhibitor). We found that SP (Jnk inhibitor) and PDTC (NFκB inhibitor) significantly reduced MN migration towards citENA-78/CXCL5. The other inhibitors used had no significant effect upon citENA-78/CXCL5 mediated MN chemotaxis (n = number of independent experimental replicates).

Progress and Accomplishments: Previously, we have shown that citrullination converts ENA-78/CXCL5 from a neutrophil recruiter to a MN recruiter. In this study, we investigated the signaling pathways involved in MN recruitment by

citENA78/CXCL5. Rh ENA78/CXCL5 was citrullinated by incubation with rhPAD4 enzyme. To confirm the citrullination sites, citENA78/CXCL5 was analyzed using liquid chromatography-tandem mass spectrometry (LC-MS/MS). To determine the signaling pathways involved, MN chemotaxis assay was performed with citENA78/CXCL5 in modified Boyden chambers with chemical signaling inhibitors. MNs that were also transfected with JNK siRNA. Three mutants (R45K, R48K and R45/48K) of rhENA78/CXCL5 were generated by transmutation of arginines to lysines and were used in MN chemotaxis assays. To assess citENA78/CXCL5-induced MN migration *in vivo*, a mouse subcutaneous air pouch model was used. The exudates from the air pouch were collected after 24 hours and immunofluorescence was performed to detect MNs/macrophages using anti-F4/80 antibody. MNs were stimulated with citENA78/CXCL5 for 15 minutes and Western blots were performed to evaluate phosphorylation of signaling molecules. We also assessed the crosstalk between the signaling pathways after incubating with chemical signaling inhibitors before citENA78/CXCL5 stimulation.

We found that citENA78/CXCL5 plays an important role in MN migration *in vivo* in the air pouch inflammatory model. Our data suggest that citENA78/CXCL5 induces JNK and NFκB signaling pathways with JNK upstream of NFκB. Therefore, targeting citENA78/CXCL5 and its signaling pathways may be a novel approach to treat MN-dependent diseases in which citENA-78/CXCL5 is expressed.

Current Objectives: **Specific Aim 3: To identify if patients with RA produce antibodies to citrullinated vs. noncitrullinated chemokines.**

Major task III: To examine autoantibody formation to citrullinated chemotactic factors in RA and rat adjuvant induced arthritis.

Subtask 1: Sera will be obtained from RA, OA, or NL individuals and assayed against citrullinated vs. noncitrullinated chemokines to determine if autoantibodies are made.

Subtask 2: Citrullinated chemokines will be adsorbed out of RA serum to determine how much reactivity for citrullinated antigens remains.

Summary of Results: Our data suggested that citrullination of nuclear proteins may account for much of the citrullination seen in RA SF and RA PB. To investigate this further, we examined the possibility that Id1 may be a significant contributor of citrullination in RA tissues. Therefore, we performed many of our immunoassays to citrullinated chemokines with citrullinated Id1 for comparison. ELISA analysis of RA SFs showed that the levels of total citrullinated antigens were significantly reduced upon immunodepletion of Id1. Western blot (WB) analysis of immunoprecipitated Id1 from homogenized RA STs showed that a significant portion of the total Id1 was in the modified form. We were able to detect citId1 via the cit-ELISA, and to verify by another method that we could citrullinate Id1 successfully, we performed liquid chromatography coupled with tandem mass spectrometry (LC/MS-MS) on modified Id1. We could identify modified arginines after incubation of recombinant Id1 with PAD enzyme by detecting the neutral loss of isocyanic acid (HNCO; -43Da), much like we observed with citENA-78/CXCL5. These are diagnostic marker ions for citrullination and confirm that Id1 has been modified by PAD enzyme. Immunodot blot (IDB) analysis of mouse anti-human Id1 antibody (previously used in immunodepletion and immunoprecipitation) showed positive signals from both citId1 and noncitId1, suggesting that this binding epitope was not modified by citrullination. IDB analysis of the patient sera showed robust signals for citId1, and weak but significant signals for citENA-78/CXCL5 (not shown in figure because the signal compared to citId1 is very low), from multiple RA patient PB sera, displaying a four-fold increase in average reactivity for citId1 as compared to NL patient PB sera. We show for the first time the presence of ACPAs with specificity to citId, and weak specificity for citENA-78/CXCL5 in RA patient PB sera, and propose citId1, and to a lesser extent citENA-78/CXCL5 as novel autoantigen candidates in RA.

Progress and Accomplishments: Id1 is a nuclear transcription factor actively transcribed in endothelial progenitor cells and in cells that exhibit hyperproliferative responses such as synovial fibroblasts (2). Previously, we identified Id1 as an angiogenic and chemotactic factor expressed in RA STs and upregulated in RA SFs. Although it is a relatively small protein of approximately 16 kDA, Id1 contains 10 modifiable arginines. As a variety of citrullinated proteins are known to bind to anti-citrullinated protein antibodies (ACPAs), we investigated citrullinated Id1 (citId1) as a potential autoantigen in RA and compared its potential ACPA producing activity compared to citENA-78/CXCL5, known to be expressed in RA (figure 1). Previously, RA SFs were immunodepleted of ENA-78/CXCL5 and measured by ELISA using anti-modified citrulline (AMC) antibody for total citrullinated antigens pre and post depletion. ENA-78/CXCL5 was also immunoprecipitated from homogenized RA STs and analyzed by WB using anti-human ENA-78/CXCL5 or AMC antibodies. In this study, we performed similar assays upon Id1 as this protein is a nuclear protein and can be deiminated similar to other nuclear proteins (i.e. histones), making it a suitable molecule for comparison to ENA-78/CXCL5. CitId1 was prepared *in vitro* from recombinant human (rh) Id1 by incubation with rh peptidyl arginine deiminase 4 (PAD4); noncitrullinated Id1 (noncitId1) was prepared identically without rhPAD4. To confirm the citrullination sites, citId1 and noncitId1 were analyzed much like we did previously for ENA-78/CXCL5, by using LC-MS/MS. To test the presence of ACPAs to citENA-78/CXCL5 and citId1, NL and RA patient PB sera immunodepleted of rheumatoid factor (RF) were analyzed using IDB analysis. CitENA-78/CXCL5 and citId1 as well as noncitENA-78/CXCL5 and noncitId1 were dotted onto nitrocellulose membranes, blocked, and incubated in the patient sera. Bovine serum albumin (BSA) and citBSA were used as antigen controls; anti-human Id1 antibody and rh IgG were used as sera controls. We found that citENA-78/CXCL5 only weakly bound ACPAs in RA SF and RA PB, whereas citId1 reacted much more strongly to ACPAs in the RA SF and especially RA PB, suggesting that the modified forms of these proteins may serve as potential autoantigens in RA.

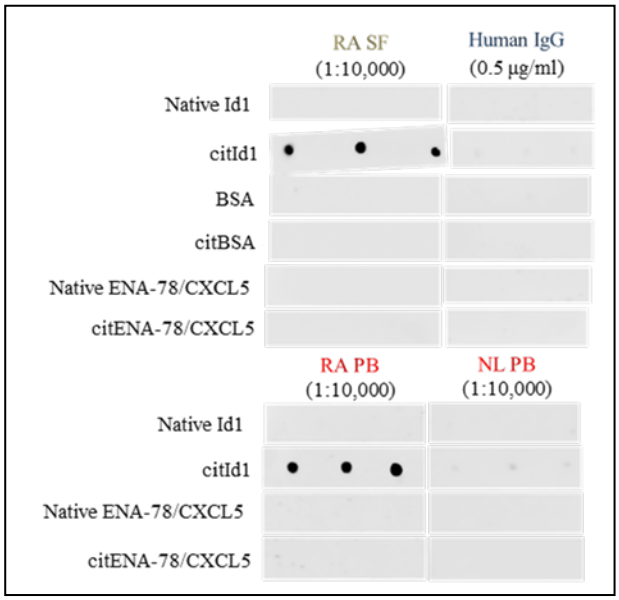

Figure 3. *Analysis of ACPAs to citId1*. RA SFs and sera obtained from NL individuals and RA patients were assayed for autoantibodies to citrullinated Id1 (citId1) by immune dot blot analysis. Before performing the dot blots, all sera and SFs were immunodepleted of rheumatoid factor (RF) by incubating specimens with anti-IgM coupled beads. Immunodepletion of RF was confirmed by measuring the amounts of RF before and after treatment with the anti-IgM coupled beads. Antigens were blotted onto nitrocellulose membrane (NCM) and blocked with 5% goat serum in TBST buffer. NCM was incubated overnight with RA SF or sera diluted 1:10,000 in TBST. Blots were washed and incubated with a secondary antibody [horseradish peroxidase conjugated goat anti-human IgG (Millipore)] diluted 1:10,000 in TBST for detection of ACPAs by digital image analysis. Imaging was done using electrochemiluminescence (ECL) reagent after 5 minute incubation. Exposure time was 1 minute for all blots. As shown in the representative blots, we found positive results for ACPA reactivity for citId1, but not native Id1, in RA SF and RA PB, but not in the PB of NL (healthy) subjects. To control for non-specific antibody binding, control antigens including native Id1, BSA, citBSA, native ENA-78/CXCL5 and citENA-78/CXCL5 were tested on the same NCM as citId1. Human IgG served as a control for non-specific serum antibody binding. Control blots showed no significant evidence of ACPAs or antibody binding reactivity in RA SF, RA PB or in NL PB. We found 4/9 RA PBs and 0/5 NL PBs that were significantly immunopositive for citId1 (all samples were run in triplicate).

4. Key Research Accomplishments

- CitENA-78/CXCL5 was significantly higher in RA sera and SFs than NL sera and OD including OA SFs, respectively.

- A strong correlation was found between the amount of citENA-78/CXCL5 and C-reactive protein or erythrocyte sedimentation rate (ESR) in RA SFs.

- Our conclusions for the first year of experiments is that citENA-78/CXCL5 can be detected in RA tissues and is highly correlated with RA disease activity.

- We have generated mutants for our project (as proposed) and now have constructs of ENA-78/CXCL5 that are non-mutated, and two others that have the arginine replaced by a lysine residue (Origene). These mutant forms will be tested against non-mutated ENA-78/CXCL5 to examine its cell recruitment activity in citrullinated and non-citrullinated forms.

- Mice have been immunized with citENA-78/CXCL5 to produce a monoclonal antibody to the modified form of this pro-inflammatory chemokine. If successful in isolating the B-Cell clone, we will isolate and use these antibodies to examine the expression and function of citENA-78/CXCL5 in RA tissues.

- CitENA78/CXCL5 plays an important role in MN migration *in vivo* in the air pouch inflammatory model. Our data suggest that citENA78/CXCL5 induces JNK and NFκB signaling pathways with JNK upstream of NFκB. Targeting citENA78/CXCL5 and its signaling pathways may be a novel approach to treat MN-dependent diseases.

- CitR45K and citR48K mutations is citENA-78/CXCL5 significantly reduced MN chemotaxis, suggesting that citENA78/CXCL5-induced MN migration is dependent, at least partially, on both citrulline residues.

- IDB analysis of the patient sera showed robust signals for citId1, and weak but significant signals for citENA-78/CXCL5 (not shown in figure because the signal compared to citId1 is very low), from multiple RA patient PB sera, displaying a four-fold increase in average reactivity for citId1 as compared to NL patient PB sera.

- We show for the first time the presence of ACPAs with weak specificity to citENA-78/CXCL5 and robust binding activity for citId1 in RA patient PB sera, and propose ENA-78/CXCL5 and especially citId1 as a novel autoantigen candidate in RA.

5. Conclusion

Citrullinated chemokine concentrations were measured by enzyme linked immunosorbent assay in RA and NL sera and in RA, OA, and OD SFs. The correlation between the citrullinated chemokine levels and clinical data was analyzed. We found that citENA-78/CXCL5 was significantly higher in RA sera and SFs than NL sera and OD including OA SFs, respectively. A strong correlation was found between the amount of citENA-78/CXCL5 and C-reactive protein or erythrocyte sedimentation rate in RA SFs. Our conclusions for the first two years of experiments is that citENA-78/CXCL5 can be detected in RA tissues and is highly correlated with RA disease activity. Also, citENA78/CXCL5 plays an important role in MN migration in vitro and in vivo and signals via the JNK and NFκB signaling pathways. Finally, we show for the first time the presence of ACPAs with specificity to citId1, and with weak specificity for citENA-78/CXCL5 in RA patient PB sera. Taken together, evidence is strong for citrullination being integral to inflammation and the pathogenesis of RA.

6. Publications, Abstracts and Presentations

Peer-reviewed manuscripts:

1. Yoshida Y, Korchynskyi O, Tak PP, Isozaki T, Ruth JH, Campbell PL, Baeten DL, Gerlag DM, Amin MA, Koch AE: Citrullination of ENA-78/CXCL5 results in conversion from a non-monocyte recruiting to a monocyte recruiting chemokine. *Arthritis Rheumatol*. 66:2716-27, 2014.
2. Edhayan G, Ha CM, Isozaki T, Amin MA, Ohara RA, Morgan R, Campbell PL, Haines GK III, Arbab S, Friday S, Stinson WA, Fox DA, Ruth JH: Inflammatory Properties of Inhibitor of DNA Binding 1 as a Unique Fibroblast Derived Nuclear Protein. *Submitted*.
3. Ohara RA, Lepore N, W. Stinson WA, Edhayan G, Campbell PL, Arwani S, Morgan RL, Ruth JH, Koch AE, Fox DA, Amin MA: Citrullinated ENA78/CXCL5 Induces Monocyte Migration via JNK and NFκB Signaling Pathways. *In preparation.*

Abstracts accepted to national meetings:

1. Yoshida K, Campbell PL, Amin MA, Koch AE, Fox DA, Ruth JH: Citrullination of ENA-78/CXCL5 changes its receptor affinity from CXCR2 to CXCR1 and induces monocyte migration. *Arthritis Rheum*. 65 S10:327, 2013.
2. Edhayan G, Ha CM , Ohara RA, Isozaki T, Amin MA, Arbab AS, Tsou PS, Campbell PL, Schiopu E, Khanna D, Morgan R, Friday SC, Fox DA, Ruth JH: Inflammatory Properties of Inhibitor of DNA Binding 1 as a Unique Fibroblast Derived Nuclear Protein. *Arthritis Rheumatol*. 66 S10:863, 2014.
3. Ohara RA, Edhayan G, Ha CM, Amin MA, Arbab AS, Campbell PL, Fox DA, Ruth JH: Evidence for citrullination of the nuclear transcription factor Inhibitor of DNA Binding 1 (Id1) in Rheumatoid Arthritis. *Arthritis Rheumatol*: 66 S10:189, 2014.
4. Ohara RA, Edhayan G, Stinson WA, Campbell PL, Remmer HA, Amin MA, Fox DA, Ruth JH: Evidence for Citrullinated Inhibitor of DNA Binding 1 (Id1) as a Novel Autoantigen Candidate in Rheumatoid Arthritis. *Arthritis Rheumatol* In press.
5. Edhayan G, Ha CM, Ohara RA, Isozaki T, Amin MA, Arbab AS, Campbell PL, Morgan R, Stinson WA, Friday SC, Fox DA, Ruth JH: Inhibitor of DNA Binding 1 as a Fibroblast Derived Inflammatory Angiogenic Agonist in Rheumatoid Arthritis. *Arthritis Rheumatol* In press.
6. Ohara RA, Lepore N, W. Stinson WA, Edhayan G, Campbell PL, Arwani S, Morgan RL, Ruth JH, Koch AE, Fox DA, Amin MA: Citrullinated ENA78/CXCL5 Induces Monocyte Migration via JNK and NFκB Signaling Pathways. *Arthritis Rheumatol* In press.

7. Inventions, Patents and Licenses

Nothing to report.

8. Reportable outcomes

- We developed an ELISA that can successfully detect citrullinated chemokines in RA tissues.
- We developed a Western blotting technique that can successfully detect citrullinated chemokines in RA tissues.
- We can correlate RA disease severity with citENA-78/CXCL5 concentrations in RA SF.

- We found that citENA78/CXCL5 plays an important role in MN migration *in vivo* in the air pouch inflammatory model. Our data suggest that citENA78/CXCL5 induces JNK and NFκB signaling pathways with JNK upstream of NFκB. Targeting citENA78/CXCL5 and its signaling pathways may be a novel approach to treat MN-dependent diseases.

- We discovered that alteration of arginine residues R45K and R48K (by replacing them with lysine residues) results in a significant reduction in citENA-78/CXCL5 MN chemotaxis. This suggests that both arginine residues are responsible for conversion of ENA-78/CXCL5 from a normally neutrophil recruiting chemokine into a monocyte chemotactic factor after deimination.

- ACPAs can be detected in RA PB for ENA-78/CXCL5 and especially for citId1 in RA PB and SF suggenting that ENA-78/CXCL5 and especially citId1 may serve as autoantigens in RA.

9. Other Achievements

- We found that a nuclear regulatory factor Id1 protein can be deiminated and has robust binding for ACPAs in RA SF and especially RA PB. We also have preliminary evidence that Id1 may regulate chemokine expression from RA fibroblasts.

10. References

1. Yoshida Y, Korchynskyi O, Tak PP, Isozaki T, Ruth JH, Campbell PL, Baeten DL, Gerlag DM, Amin MA, Koch AE: Citrullination of ENA-78/CXCL5 results in conversion from a non-monocyte recruiting to a monocyte recruiting chemokine. *Arthritis Rheumatol*. 66:2716-27, 2014.

2. Edhayan G, Ha CM, Isozaki T, Amin MA, Ohara RA, Morgan R, Campbell PL, Haines GK III, Arbab S, Friday S, Stinson WA, Fox DA, Ruth JH: Inflammatory Properties of Inhibitor of DNA Binding 1 as a Unique Fibroblast Derived Nuclear Protein. *Submitted*.

11. Appendices

Please see manuscripts (references 1 and 2) enclosed.

Quad/Gantt chart

TIMETABLE FOR RESEARCH PROGRAM			
	YEAR 01	YEAR 02	YEAR 03
SPECIFIC AIM #1	COMPLETED: Synovial fluids and sera will be obtained from patients with RA, OA or other diseases and assayed for key citrullinated and non-citrullinated chemokines thought to be important in the pathogenesis of RA.	COMPLETED: Synovial tissue will be obtained from RA, OA, or NL joints, homogenized and assayed for citrullinated and non-citrullinated chemokines.	
SPECIFIC AIM #2	COMPLETED: Leukocyte chemotaxis assays, modifying chemokines containing ELR motif and mass spec analysis, site directed mutagenesis of chemokines.	COMPLETED: Signal transduction analysis of endothelial cells and leukocytes.	*In vitro* Angiogenesis assays and Matrigel plug assay (if needed)
SPECIFIC AIM #3		75% COMPLETE: Sera obtained from RA, OA, or NL individuals will be assayed against citrullinated vs. non-citrullinated chemokines to determine if autoantibodies are made.	Citrullinated chemokines will be adsorbed out of RA serum to determine how much reactivity for citrullinated antigens remains.
SPECIFIC AIM #4		COMPLETED: Determine the inflammatory effect of injecting citrullinated chemokines vs. native chemokines into normal rodent knees.	50% COMPLETE: Perform rat adjuvant induced arthritis and determine whether citrullinated chemokines and antibodies to these chemokines are present before and during development of arthritis.

ARTHRITIS & RHEUMATOLOGY
Vol. 66, No. 10, October 2014, pp 2716–2727
DOI 10.1002/art.38750

Citrullination of Epithelial Neutrophil–Activating Peptide 78/CXCL5 Results in Conversion From a Non–Monocyte-Recruiting Chemokine to a Monocyte-Recruiting Chemokine

Ken Yoshida,[1] Olexandr Korchynskyi,[2] Paul P. Tak,[2] Takeo Isozaki,[1] Jeffrey H. Ruth,[1] Phillip L. Campbell,[1] Dominique L. Baeten,[2] Danielle M. Gerlag,[2] M. Asif Amin,[1] and Alisa E. Koch[3]

Objective. **To examine whether the citrullinated chemokines epithelial neutrophil–activating peptide 78 (ENA-78)/CXCL5, macrophage inflammatory protein 1α/CCL3, and monocyte chemotactic protein 1/CCL2 are detected in the biologic fluid of patients with rheumatoid arthritis (RA), and if so, to determine the biologic activities of these chemokines.**

Methods. **Recombinant human chemokines were citrullinated by peptidylarginine deiminase. Enzyme-linked immunosorbent assays were performed to measure the concentrations of citrullinated chemokines in sera from patients with rheumatoid arthritis (RA) and normal individuals and in synovial fluid from patients with RA, patients with osteoarthritis (OA), and patients with other inflammatory rheumatic diseases. The correlation between the citrullinated chemokine levels and clinical data was analyzed. Monocyte and neutrophil chemotaxis assays were performed, and native (non-citrullinated) or citrullinated ENA-78/CXCL5 was injected into mouse knees to evaluate the biologic activities of these chemokines.**

Results. **The concentration of citrullinated ENA-78/CXCL5 was significantly higher in RA sera and SF than in normal sera and in SF from patients with other rheumatic diseases including OA. In RA SF, a strong correlation between the amount of citrullinated ENA-78/CXCL5 and the C-reactive protein level or the erythrocyte sedimentation rate was observed. Citrullinated ENA-78/CXCL5 induced monocyte chemotaxis via CXCR1 and CXCR2, while noncitrullinated ENA-78/CXCL5 did not. In a mouse model of inflammatory arthritis, citrullinated ENA-78/CXCL5 induced more severe inflammation and recruited more monocytes than did noncitrullinated ENA-78/CXCL5.**

Conclusion. **Citrullinated ENA-78/CXCL5 is highly correlated with RA disease activity and, unlike noncitrullinated ENA-78/CXCL5, recruits monocytes. These results indicate that citrullinated ENA-78/CXCL5 may exert previously unrecognized inflammatory properties in RA by recruiting monocytes to inflamed joint tissue.**

Rheumatoid arthritis (RA) is a chronic inflammatory disorder characterized by the infiltration of inflammatory cells into synovial tissue and synovial fluid (SF) (1). Anti–cyclic citrullinated peptide (anti-CCP) antibodies are present in the sera of nearly 70% of patients with RA and have become key diagnostic markers for this disease (2). Citrulline residues in target antigens are essential in the formation of anti–citrullinated peptide/protein antibody epitopes (3,4). These epitopes result from citrullination, a posttransla-

Supported by the Office of Research and Development, Medical Research Service, Department of Veterans Affairs and by the Frederick G. L. Huetwell and William D. Robinson, MD, Professorship in Rheumatology at the University of Michigan (awarded to Dr. Koch).

[1]Ken Yoshida, MD, PhD, Takeo Isozaki, MD, PhD, Jeffrey H. Ruth, PhD, Phillip L. Campbell, BA, M. Asif Amin, MD: University of Michigan, Ann Arbor; [2]Olexandr Korchynskyi, PhD, Paul P. Tak, MD, PhD, Dominique L. Baeten, MD, PhD, Danielle M. Gerlag, MD, PhD: University of Amsterdam, Amsterdam, The Netherlands; [3]Alisa E. Koch, MD: Department of Veterans Affairs Medical Center, Ann Arbor, and University of Michigan, Ann Arbor.

Drs. Yoshida and Korchynskyi contributed equally to this work.

Address correspondence to Alisa E. Koch, MD, University of Michigan Medical School, Ann Arbor, MI 48109-2200. E-mail: aekoch@umich.edu.

Submitted for publication June 20, 2013; accepted in revised form June 12, 2014.

tional modification of arginine. Peptidylarginine deiminase (PAD) enzymes are calcium-dependent enzymes that catalyze citrullination of target proteins by converting arginine to citrulline (5). Five PAD family members, PAD type 1 (PAD1), PAD2, PAD3, PAD4, and PAD6, have been identified in many types of tissue, including synovial tissue, and in human leukocytes (6).

Chemokines play an important role as monocyte and polymorphonuclear neutrophil (PMN) recruiters in the setting of RA synovitis and tissue destruction (7,8). Chemokines are classified into 4 subfamilies based on the number and spacing of their first cysteine residues in the primary amino acid sequence (9). These chemokine families are designated as CXC, CC, C, and CX_3C. The CXC chemokines are further divided into 2 subgroups based on whether the Glu-Leu-Arg (ELR) motif precedes the first cysteine residue. Epithelial neutrophil–activating peptide 78 (ENA-78)/CXCL5, a CXC chemokine, is an 8.3-kd protein with 78 amino acids containing 4 cysteine residues positioned identically to those of interleukin-8 (IL-8/CXCL8) (10). We previously observed that the concentration of ENA-78/CXCL5, which is associated with neutrophil recruitment, is significantly higher in RA SF compared with osteoarthritis (OA) SF or SF from patients with other forms of arthritis (11). In addition, we demonstrated that neutralization of ENA-78/CXCL5 ameliorated the severity of adjuvant-induced arthritis in a rat model (12). These findings support the notion that ENA-78/CXCL5 is important in the pathogenesis of RA.

Although the presence of citrullinated proteins such as fibrinogen, α-enolase, and vimentin in RA has been reported (4,13–15), citrullinated chemokines have not yet been detected in RA. We chose to examine chemokines, because they are biologically relevant joint proteins. Several chemokines are highly expressed in the joints of patients with RA, and PAD2 and PAD4 are mainly present in synovial tissue. The expression levels of these PADs are correlated with inflammation, thickness of the synovial lining layer, and vascularity (16). These observations support the hypothesis that citrullinated chemokines may be present in rheumatic joints.

We compared the presence of citrullinated ENA-78/CXCL5, citrullinated macrophage inflammatory protein 1α (MIP-1α)/CCL3, and citrullinated monocyte chemotactic protein 1 (MCP-1)/CCL2 in the biologic fluid of patients with RA with that in the biologic fluid of patients with other arthritic diseases, using a newly developed enzyme-linked immunosorbent assay (ELISA) system, and examined the biologic activity of these chemokines in vitro and that of ENA-78/CXCL5 in vivo.

PATIENTS AND METHODS

Patients and normal control subjects. Serum samples were obtained from 11 patients with RA and 15 normal control subjects, and SF samples were obtained from 20 patients with RA, 15 patients with OA, and 13 patients with other inflammatory rheumatic diseases, including gout (n = 4), pseudogout (n = 2), psoriatic arthritis (n = 1), spondyloarthritis (n = 3), Behçet's disease (n = 1), Lyme disease (n = 1), and unclassified arthritis (n = 1). Rheumatoid factor (RF) was immunodepleted from RA sera and SF using goat anti-human IgM (μ-chain specific) agarose (Sigma-Aldrich) prior to measuring citrullinated chemokines by ELISA. All samples were obtained after approval by the Institutional Review Board and provision of informed consent by the subjects.

Chemokine DNA cloning. Full-length ENA-78/CXCL5 complementary DNA (cDNA) (NCBI accession no. NM_002994) was obtained from Open Biosystems. We generated cDNA libraries for MCP-1/CCL2 and MIP-1α/CCL3 from primary synovial fibroblasts derived from patients with RA. The cDNA fragments encoding mature proteins were amplified by polymerase chain reaction (PCR) using primers with an incorporated *Nco* I restriction site in the forward primers and with 6 codons encoding histidines followed by a stop codon and the *Eco* RI restriction site in the reverse primers (Primer Express software; Applied Biosystems). The primers used are as follows (forward and reverse, respectively): for ENA-78/CXCL5, 5′-TAATCCATGGGAGCTGGTCCTGCCGCTGCTGT-3′ and 5′-TAAGAATTCTCAGTGATGGTGATGGTGATGGTTTTCCTTGTTTCCACCGT-3′; for MIP-1α/CCL3, 5′-TAATCCATGGGAGCTGACACGCCGACCGCCTG-3′ and 5′-TAAGAATTCTCAGTGATGGTGATGGTGATGGGCACTCAGCTCCAGGTCGC-3′; for MCP-1/CCL2, 5′-TAATCCATGGGACAGCCAGATGCAATCAATGCC-3′ and 5′-TAAGAATTCTCAGTGATGGTGATGGTGATGAGTCTTCGGAGTTTGGGTTTG-3′. *Nco* I/*Eco* RI–flanked PCR fragments containing a C-terminus 6×His tag were initially cloned into a pQE-TriSystem Vector (Qiagen). All sequences were verified using BigDye Terminator sequencing (Life Technologies). For optimization of mammalian expression, inserts containing a C-terminus 6×His tag were further cloned into the mammalian expression vector pcDEF (17).

Transfection of HEK 293T cells and purification of recombinant human chemokines. All mammalian expression vectors were transfected into HEK 293T cells using polyethylenimine (Polysciences) to collect 6×His-tagged chemokines from cellular lysates prepared with 1% Triton X-100. Chemokines (6×His tagged) from HEK 293T cell lysates were purified with ProBond Nickel beads (Life Technologies), rinsed extensively with 10 m*M* imidazole, and eluted gradually with 50–200 m*M* imidazole. The quality and quantity of expressed recombinant proteins were assessed with appropriate DuoSet ELISA kits (R&D Systems) specific for these proteins and with colloidal Coomassie staining after sodium dodecyl sulfate–polyacrylamide gel electrophoresis resolution.

In vitro citrullination of chemokines. After the concentration of purified chemokines was measured using DuoSet ELISA kits, 100 microliters of purified recombinant human chemokine (~100 ng/ml) was incubated with 0.5 units of rabbit

skeletal muscle PAD (Sigma-Aldrich) in 40 m*M* Tris HCl, pH 7.6, 10 m*M* $CaCl_2$, and 2.5 m*M* dithiothreitol for 2 hours at 37°C. Deimination was stopped by chelating the calcium with 25 m*M* EDTA. These citrullinated chemokines were subsequently used as standards for ELISA of citrullinated chemokines. Alternatively, 5 μM recombinant human ENA-78 (rhENA-78)/CXCL5, recombinant human MIP-1α/CCL3, or recombinant human MCP-1/CCL2 (OriGene) was incubated with rabbit skeletal PAD (250 n*M*) at enzyme:substrate molar ratios of 1:20 in 40 m*M* Tris HCl with 2 m*M* $CaCl_2$ (pH 7.4) for 1.5 hours at 37°C. Deimination was stopped with 0.1% trifluoroacetic acid (TFA). These citrullinated chemokines were used in both in vitro chemotaxis assays and in vivo experiments. Citrullination of rhENA-78/CXCL5 was confirmed by Western blotting (18). For detection of citrullinated protein, citrulline residues were chemically modified to form a ureido group adduct before addition of an anti–modified citrulline antibody (Millipore) according to the manufacturer's protocol, which enables detection of citrulline residues independent of neighboring amino acid sequences (19). The diagnostic +1Da mass shift occurring upon citrullination was identified by liquid chromatography tandem mass spectrometry (MS Bioworks) (20).

Sandwich ELISA for citrullinated chemokines. An ELISA was designed to determine the concentrations of citrullinated chemokines in biologic fluid. Ninety-six–well plates (Thermo Fisher Scientific) were coated overnight at room temperature with mouse anti-human ENA-78/CXCL5, mouse anti-human MCP-1/CCL2, or goat anti-human MIP-1α/CCL3 (R&D Systems). Between each step, the plates were washed with wash buffer (0.05% Tween 20 in phosphate buffered saline [PBS]). The plates were blocked with 1% bovine serum albumin (BSA) in PBS for 1 hour at room temperature and incubated with serum, SF, or standards for 2 hours at room temperature. Citrullinated recombinant human chemokines and native (noncitrullinated) recombinant human chemokines purified from the transfected HEK 293T cells were used as standards and negative controls, respectively, for the ELISA. The samples were crosslinked onto the plates with 1% glutaraldehyde in PBS for 30 minutes at room temperature.

The plates were then incubated with 0.2*M* Tris HCl (pH 7.8) for 30 minutes at room temperature to block the crosslinking. The plates were then incubated overnight at 37°C in a citrulline-modification solution consisting of 2 parts solution A (0.025% [weight/volume] $FeCl_3$, 4.6*M* H_2SO_4, and 3.0*M* H_3PO_4), 1 part solution B (1% diacetylmonoxime, 0.5% antipyrine, and 1*M* acetic acid), and 1 part H_2O (18). The plates were incubated for 2 hours at room temperature with rabbit anti–modified citrulline (Millipore), diluted 1:2,500 in PBS containing 1% BSA. The plates were incubated for 2 hours at room temperature with horseradish peroxidase (HRP)–conjugated swine anti-rabbit IgG (Dako), diluted 1:1,000 in PBS containing 1% BSA. Biotin-Tyramide Reagent (PerkinElmer), diluted 1:1,000 in 0.05*M* Tris (base pH 8.5), was added, followed by HRP-conjugated streptavidin. The plates were developed using tetramethylbenzidine, development was stopped with 2*N* H_2SO_4, and the plates were read on a microplate reader at 450 nm. Serum and SF chemokine concentrations were also measured using DuoSet ELISA kits.

In vitro monocyte and polymorphonuclear neutrophil (PMN) chemotaxis assays. Monocytes and PMNs were isolated from normal human peripheral blood. Monocyte and PMN chemotaxis assays were performed using 48-well modified Boyden chambers (Neuro Probe) as described previously (21,22). Noncitrullinated chemokines (OriGene), citrullinated chemokines, and reaction buffer consisting of 40 m*M* Tris HCl, 2 m*M* $CaCl_2$, 250 n*M* rabbit skeletal PAD, and 0.1% TFA were diluted by PBS with calcium and magnesium in the same manner and tested for chemotaxis. The composition of the reaction buffer that contained PAD enzymes was the same as the composition of the stock solution of citrullinated chemokines. PBS with calcium and magnesium and fMLP (100 n*M*) (Sigma-Aldrich) were used as negative and positive stimuli, respectively. For the inhibitor studies, monocytes (2.5×10^6/ml) were pretreated with 500 ng/ml pertussis toxin (Sigma-Aldrich), which is a G protein–coupled receptor antagonist, 10 μg/ml anti-CXCR1, anti-CXCR2, or isotype control IgG2a (R&D Systems) in PBS with calcium and magnesium for 1 hour to examine whether G protein–coupled receptors are used by citrullinated ENA-78/CXCL5 to induce monocyte chemotaxis.

Mouse model of inflammatory arthritis. Female C57BL/6 mice (8–10 weeks old) were purchased from the National Cancer Institute. The mice were divided into the following 3 treatment groups: PBS, noncitrullinated ENA-78/CXCL5 (Origene), and citrullinated ENA-78/CXCL5. The mice were anesthetized, and the knee circumference was determined by caliper measurements before intraarticular injection and calculated using the following formula: circumference $= \pi\ (a + b)/2$, where a is the laterolateral diameter and b is the anteroposterior diameter. The anesthetized mice received 20 μl/knee joint of PBS, noncitrullinated ENA-78/CXCL5 (16 ng), or citrullinated ENA-78/CXCL5 (16 ng). In all of the mice, circumference measurements were obtained in a blinded manner 24 hours after the intraarticular injection.

Hematoxylin and eosin (H&E) and immunofluorescence staining. Mouse knee joints embedded in OCT compound were frozen and cut (10 μm). H&E staining was performed as described previously (23). Immunofluorescence staining was performed on cryosections from mouse knee joints to determine monocyte/macrophages, using rat anti-mouse F4/80 antibodies (GeneTex) at 1 μg/ml as primary antibody and Alexa Fluor 555–conjugated goat anti-rat IgG (Life Technologies) at a dilution of 1:200 as secondary antibody. The method of immunofluorescence staining has been described previously (21). The number of F4/80-positive monocyte/macrophages was calculated as the average of the number of cells in 3 fields (400×) that showed the most remarkable infiltrates in the joint space where the injections were administered.

Statistical analysis. Statistical differences between experimental groups were determined by Student's *t*-test or one-way analysis of variance followed by Tukey's multiple comparison test for post hoc analysis. The clinical correlation between chemokine levels and clinical data was assessed by Pearson's correlation coefficient. Statistical analysis was performed with assistance from personnel at the Center for Statistical Consultation and Research at the University of Michigan. Results are expressed as the mean ± SEM. *P* values less than 0.05 were considered significant.

RESULTS

Detection of citrullinated rhENA-78/CXCL5 and verification of in vitro citrullination of ENA-78/CXCL5. As shown in Figure 1A, the standard curve of citrullinated rhENA-78/CXCL5, as determined by ELISA, demonstrated high correlation between the concentration of citrullinated rhENA-78/CXCL5 and absorbance (Figure 1A). Noncitrullinated ENA-78/CXCL5 (1000 pg/ml) was not detected by this ELISA. We then performed Western blotting to confirm that rhENA-78/CXCL5 was citrullinated in vitro. Citrullinated ENA-78/CXCL5 was recognized by anti–modified citrulline antibody, while noncitrullinated ENA-78/CXCL5 was not (Figure 1B). The diagnostic +1Da mass shift occurring upon citrullination of ENA-78/CXCL5, which has 2 arginine residues, was identified by mass spectrometry (20). The mass spectrometry data indicated that both arginine residues were detected and citrullinated (Figures 1C and D). Citrullination of MCP-1/CCL2 and MIP-1α/CCL3, which have 4 and 3 arginine residues, respectively, was also identified by mass spectrometry (data not shown).

Citrullinated chemokine concentrations in RA sera and normal control sera. To ascertain whether citrullinated chemokines were detectable in biologic fluids, we assayed serum samples obtained from patients with RA and normal control subjects, using a citrullinated chemokine sandwich ELISA. In normal control subjects and patients with RA, the mean ± SEM levels of citrullinated ENA-78/CXCL5 were 1.2 ± 0.7 pg/ml and 286 ± 68 pg/ml, respectively (Figure 2A). The levels of citrullinated MIP-1α/CCL3 in normal and RA sera were 1.2 ± 1.2 pg/ml and 624 ± 96 pg/ml, respectively (Figure 2B), and the levels of citrullinated MCP-1/CCL2 in normal and RA sera were 0.9 ± 0.5 pg/ml and 143 ± 18 pg/ml, respectively (Figure 2C). The levels of citrullinated ENA-78/CXCL5, MIP-1α/CCL3, and MCP-1/CCL2 in patients with RA were all significantly higher than the levels in normal control subjects ($P < 0.05$). The mean ± SEM concentrations of ENA-78/CXCL5

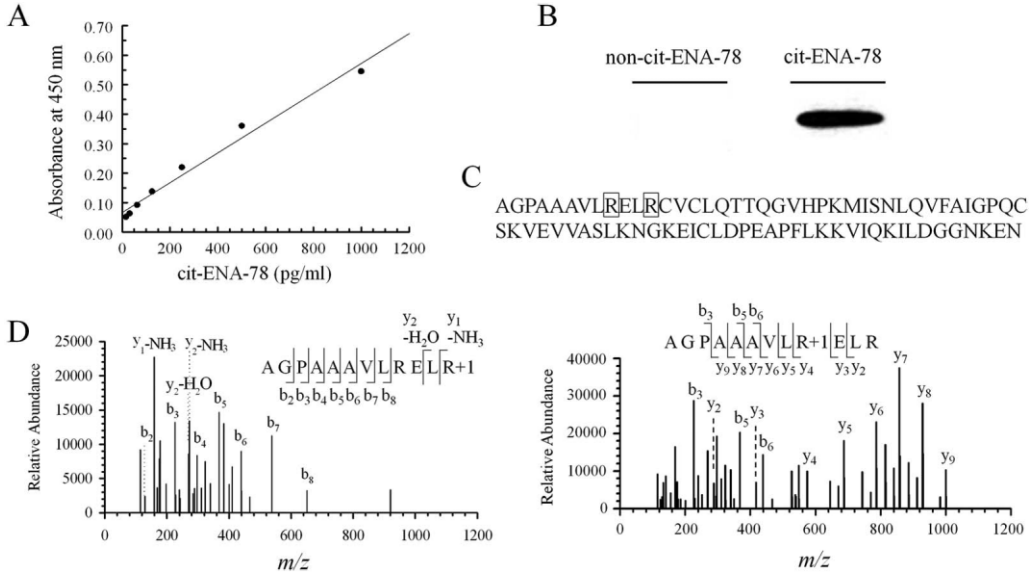

Figure 1. Detection of citrullinated recombinant human epithelial neutrophil–activating peptide 78 (ENA-78)/CXCL5 and verification of successful in vitro citrullination of ENA-78/CXCL5. **A,** Standard curve of citrullinated recombinant human ENA-78/CXCL5 as determined by enzyme-linked immunosorbent assay. Each point was determined using duplicate assays. **B,** Immunoblots showing that citrullinated recombinant human ENA-78/CXCL5 was recognized by anti–modified citrulline antibody (right) while noncitrullinated ENA-78/CXCL5 was not (left). The blot used to detect citrullinated protein was chemically modified prior to immunostaining. **C,** Amino acid sequence of ENA-78/CXCL5 (mature form 37–114). The boxed areas show the citrullinated arginines that were detected. **D,** Annotated tandem mass spectrometry (MS/MS) fragmentation spectra for the citrullinated ENA-78/CXCL5 peptides, showing the citrullinated arginine residues. Left, MS/MS spectrum confirming the presence of C-terminal citrullination at position 12 (R48) from the y_1 and y_2 ions present in the spectrum. Right, The presence of ions y_4 to y_9 in the spectrum confirms the presence of the "middle" R+1 (citrullination) at position 9 (R45). The MS/MS fragmentation data were annotated using Expert System (Max-Planck Institute of Biochemistry). The precursor ion was observed with a mass error of <1 parts per million, and the error for the fragment ions was ≤0.02 daltons.

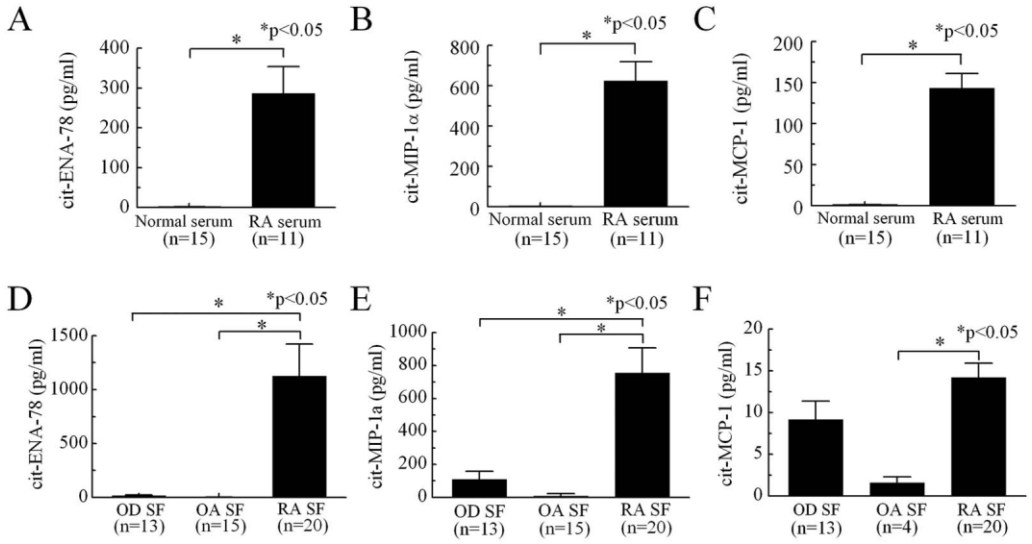

Figure 2. Expression of citrullinated chemokines in rheumatoid arthritis (RA) sera and synovial fluid (SF). Citrullinated chemokines were measured using an enzyme-linked immunosorbent assay (ELISA) in which chemokines were captured on an ELISA plate, followed by detection with anti–modified citrulline after chemical modification of citrulline residues. Rheumatoid factor was depleted from RA SF and RA sera prior to the ELISA. **A–C,** Concentrations of citrullinated epithelial neutrophil–activating peptide 78 (ENA-78)/CXCL5 (**A**), macrophage inflammatory protein 1α (MIP-1α)/CCL3 (**B**), and monocyte chemotactic protein 1 (MCP-1)/CCL2 (**C**) in normal sera and sera from patients with RA. **D–F,** Concentrations of citrullinated ENA-78/CXCL5, citrullinated MIP-1α/CCL3, and citrullinated MCP-1/CCL2 in SF from patients with other inflammatory rheumatic diseases (OD), patients with osteoarthritis (OA), and patients with RA. Bars show the mean ± SEM.

were 3,165 ± 825 pg/ml in normal sera and 3,942 ± 1,139 pg/ml in RA sera, the levels of MIP-1α/CCL3 were 230 ± 176 pg/ml and 727 ± 420 pg/ml, respectively, and the levels of MCP-1/CCL2 were 43 ± 22 pg/ml and 289 ± 271 pg/ml, respectively; none of the differences between groups were statistically significant (results not shown).

Citrullinated chemokine concentrations in SF from patients with RA, patients with OA, and patients with other rheumatic diseases. The concentrations of citrullinated chemokines in SF samples obtained from patients with RA, patients with OA, and patients with other inflammatory rheumatic diseases were measured by sandwich ELISA. The mean ± SEM concentration of citrullinated ENA-78/CXCL5 was significantly higher in SF from patients with RA (1,126 ± 297 pg/ml) than in SF from patients with OA (2.3 ± 1.0 pg/ml) and patients with other inflammatory rheumatic diseases (15 ± 9 pg/ml) ($P < 0.05$) (Figure 2D). The mean ± SEM concentration of citrullinated MIP-1α/CCL3 was also significantly higher in the SF of patients with RA (755 ± 152 pg/ml) compared with that in the SF of patients with other inflammatory rheumatic diseases (109 ± 49 pg/ml) and patients with OA (9 ± 15 pg/ml) ($P < 0.05$) (Figure 2E). Citrullinated MCP-1/CCL2 concentrations were significantly higher in RA SF (14 ± 2 pg/ml) compared with OA SF (1.6 ± 0.7 pg/ml) ($P < 0.05$) (Figure 2F).

We also used ELISA kits to measure chemokine concentrations. The mean ± SEM concentrations of ENA-78/CXCL5 were 163 ± 107 pg/ml in RA SF, 0 ± 0 pg/ml in the SF of patients with other diseases, and 19 ± 13 pg/ml in OA SF. The concentrations of MIP-1α/CCL3 were 460 ± 171 pg/ml in RA SF, 31 ± 10 pg/ml in SF from patients with other rheumatic diseases, and 75 ± 52 pg/ml in OA SF. The concentrations of MCP-1/CCL2 were 1,085 ± 398 pg/ml in RA SF, 288 ± 42 pg/ml in SF from patients with other rheumatic diseases, and 390 ± 80 pg/ml in OA SF. There were no significant differences in SF chemokine concentrations between these groups.

Positive correlation between citrullinated ENA-78/CXCL5 concentrations and the C-reactive protein (CRP) level and erythrocyte sedimentation rate (ESR) in RA SF. We analyzed the relationship between the citrullinated chemokine concentrations in SF and clinical data in patients with RA. As shown in Table 1, the clinical characteristics of these patients were as follows: mean ± SEM age 52.7 ± 3.4 years, disease duration 145.7 ± 39.2 months, ESR 38.1 ± 4.3 mm/hour, CRP level 40.5 ± 9.9 mg/liter, Disease Activity Score in 28

Table 1. Clinical characteristics of the patients with rheumatoid arthritis whose synovial fluid was studied*

Male/female, % (n = 20)	20/80
Age, years (n = 20)	52.7 ± 3.4
Disease duration, months (n = 20)	145.7 ± 39.2
Tender joint count in 28 joints (n = 13)	5.7 ± 2.1
Swollen joint count in 28 joints (n = 13)	4.5 ± 1.9
Bone erosion, yes/no, % (n = 20)	40/60
ESR, mm/hour (n = 15)	38.1 ± 4.3
CRP, mg/liter (n = 14)	40.5 ± 9.9
DAS28 (n = 12)	5.1 ± 0.4
Rheumatoid factor, units/ml (n = 10)	74.8 ± 43.2
Anti-CCP, AU/ml (n = 10)	2,296.1 ± 1,559.1

* Except where indicated otherwise, values are the mean ± SEM. ESR = erythrocyte sedimentation rate; CRP = C-reactive protein; DAS28 = Disease Activity Score in 28 joints; anti-CCP = anti–cyclic citrullinated peptide.

joints (24) 5.1 ± 0.4, tender joint count 5.7 ± 2.1, swollen joint count 4.5 ± 1.9, RF level 74.8 ± 43.2 units/ml, and anti-CCP antibody level 2,296.1 ± 1,559.1 AU/ml. As shown in Figure 3, citrullinated ENA-78/CXCL5 concentrations were significantly correlated with CRP levels ($r = 0.69$, $P < 0.05$) and the ESR ($r = 0.77$, $P < 0.05$), and citrullinated MCP-1/CCL2 concentrations were significantly correlated with the ESR ($r = 0.64$, $P < 0.05$). There was no significant correlation between the concentration of citrullinated MIP-1α/CCL3 in RA SF with the other clinical parameters examined.

Citrullinated ENA-78/CXCL5–induced monocyte migratory activity via CXCR1 and CXCR2. Under normal conditions, ENA-78/CXCL5 induces PMN migration, but it does not induce monocyte migration (10,25,26). We performed monocyte and PMN chemotaxis assays using a modified Boyden chamber, and the results showed that the fold increase in monocyte migration was significantly higher in response to citrullinated ENA-78/CXCL5 at 0.1 n*M*, 1 n*M*, and 10 n*M* (mean ± SEM 1.6 ± 0.1, 1.9 ± 0.2, and 1.9 ± 0.2, respectively) than in response to noncitrullinated ENA-78/CXCL5 and PBS (Figure 4A). We also tested various concentrations of reaction buffer in citrullinated ENA-78/CXCL5 stock solution for chemotaxis of monocytes. The reaction buffer including PAD enzymes did not induce monocyte migration at the concentrations tested. In contrast to citrullinated ENA-78/CXCL5, citrullinated MCP-1/CCL2 recruited significantly fewer monocytes at 10 n*M* and 100 n*M* than did noncitrullinated MCP-1/CCL2 (data not shown), and citrullinated MIP-1α/CCL3 tended to have the same level of monocyte-recruiting activity as noncitrullinated MIP-1α/CCL3 at 0.01–100 n*M* (data not shown).

PMN chemotaxis assays showed that noncitrullinated ENA-78/CXCL5 had significantly higher PMN chemotactic activity at 0.1 n*M* (1.5 ± 0.2) and 1 n*M* (1.6 ± 0.2) compared with PBS ($P < 0.05$), while citrullinated ENA-78/CXCL5 had significantly higher activity at 10 n*M* (1.4 ± 0.1) compared with PBS ($P < 0.05$) (Figure 4B). Thus, the fold increase in PMN

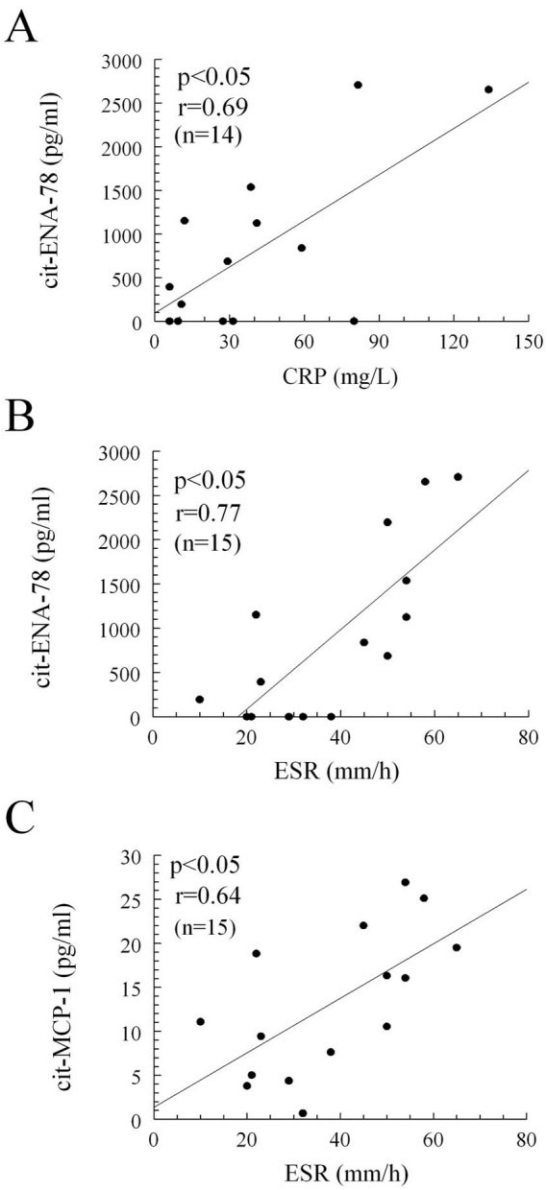

Figure 3. Correlation of clinical data with citrullinated chemokine levels in RA SF. Positive correlations between citrullinated ENA-78/CXCL5 and the C-reactive protein (CRP) level (**A**), citrullinated ENA-78/CXCL5 and the erythrocyte sedimentation rate (ESR) (**B**), and citrullinated MCP-1/CCL2 and the ESR (**C**) were observed. See Figure 2 for other definitions.

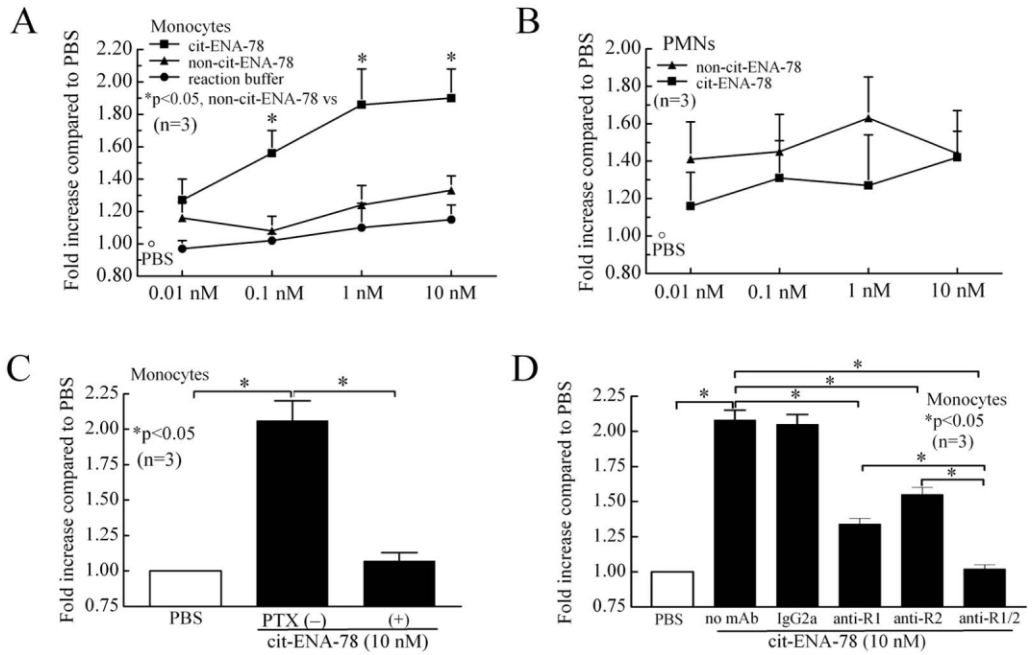

Figure 4. Monocyte recruitment by citrullinated epithelial neutrophil–activating peptide 78 (ENA-78)/CXCL5. **A,** Fold increase in monocyte migration in response to citrullinated ENA-78/CXCL5 and noncitrullinated ENA-78/CXCL5, as determined by monocyte chemotaxis assay. At 0.1 n*M*, 1 n*M*, and 10 n*M* , the response to citrullinated ENA-78/CXCL5 was significantly higher than the response to noncitrullinated ENA-78/CXCL5 and phosphate buffered saline (PBS). As controls, various concentrations of reaction buffer including peptidylarginine deiminase enzymes were tested for chemotaxis of monocytes. There was no significant difference between the response to reaction buffer and the response to PBS. The mean ± SEM fold increase in monocyte migration in response to fMLP (100 n*M*) was 4.4 ± 0.5. **B,** Fold increase in polymorphonuclear neutrophil (PMN) migration in response to citrullinated ENA-78/CXCL5 and noncitrullinated ENA-78/CXCL5, as determined by chemotaxis assay. At either 0.1 n*M* or 1 n*M*, the response to noncitrullinated ENA-78/CXCL5 was significantly higher than the response to PBS ($P < 0.05$). The response to citrullinated ENA-78/CXCL5 was lower than the response to noncitrullinated ENA-78/CXCL5, but the difference was not significant. The mean ± SEM fold increase in PMN migration in response to fMLP (100 n*M*) was 7.5 ± 2.5. **C,** Effect of pertussis toxin (PTX) on the increased monocyte migration in response to citrullinated ENA-78/CXCL5. **D,** Effect of anti-CXCR1 (anti-R1) and anti-CXCR2 (anti-R2) on the increased monocyte migration in response to citrullinated ENA-78/CXCL5. All assays were performed in quadruplicate, with 3 high-power fields (400×) counted in each replicate well. The fold increase was determined by dividing the number of cells migrated by the number of cells migrated to the negative control PBS. Values are the mean ± SEM.

migration in response to citrullinated ENA-78/CXCL5 tended to be lower than that in response to noncitrullinated ENA-78/CXCL5. However, there was no significant difference in PMN chemotaxis between noncitrullinated and citrullinated ENA-78/CXCL5.

In monocyte chemotaxis assays using pertussis toxin (a G protein–coupled receptor antagonist), anti-CXCR1, and anti-CXCR2 antibodies, the fold increase in the response to citrullinated ENA-78/CXCL5 with pertussis toxin was significantly lower (mean ± SEM 1.07 ± 0.06) compared with that without pertussis toxin (2.06 ± 0.14; $P < 0.05$) (Figure 4C). We then examined whether monocyte migration is mediated via the G protein–coupled receptors CXCR1 and CXCR2. The fold increases in the response to citrullinated ENA-78/CXCL5 with anti-CXCR1 or anti-CXCR2 antibodies were significantly lower (1.34 ± 0.04 and 1.55 ± 0.05, respectively) compared with that without the antibodies (2.05 ± 0.07), and the fold increase in the response to citrullinated ENA-78/CXCL5 with a combination of anti-CXCR1 and anti-CXCR2 antibodies was significantly lower (1.02 ± 0.03) compared with that without the antibodies, with anti-CXCR1, or with anti-CXCR2 ($P < 0.05$). IgG2a was used as an isotype-matched control monoclonal antibody that did not inhibit monocyte migration (Figure 4D). These results indicated that citrullinated ENA-78/CXCL5 induced monocyte migration via CXCR1 and CXCR2.

Citrullinated ENA-78/CXCL5–enhanced induction of inflammatory arthritis and recruitment of monocyte/macrophages in vivo. To test the inflammatory activity of citrullinated ENA-78/CXCL5 in vivo, we

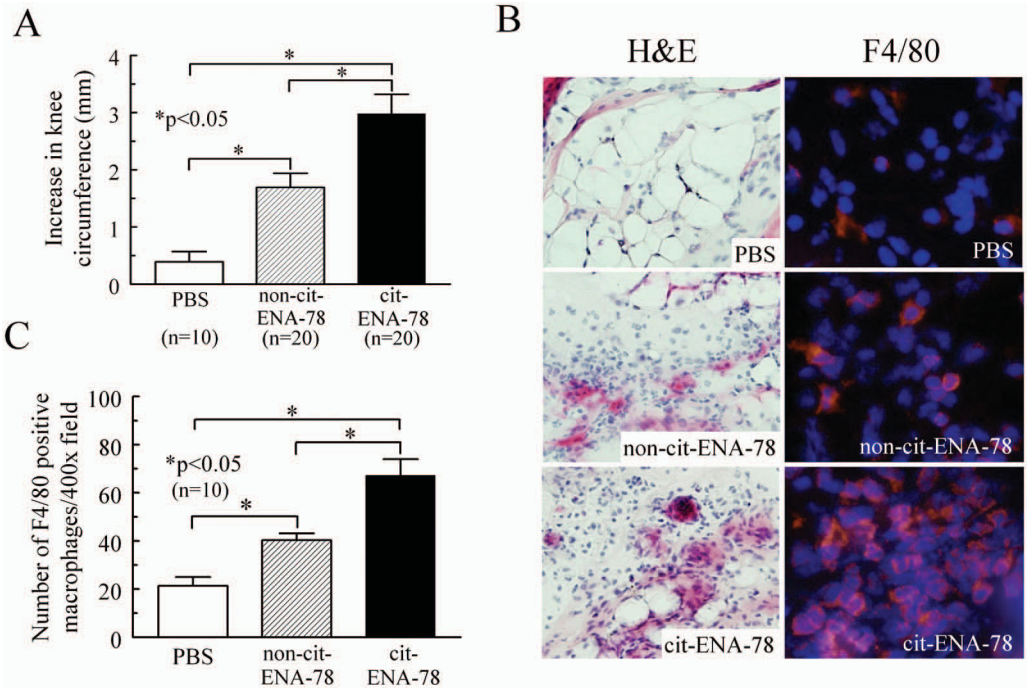

Figure 5. Effect of citrullinated ENA-78/CXCL5 in vivo. The knees of female C57BL/6 mice were injected intraarticularly with PBS, noncitrullinated ENA-78/CXCL5, or citrullinated ENA-78/CXCL5 to induce inflammation. **A,** Circumference of the mouse knees 24 hours after administration of the intraarticular injections. The increases in knee circumference were significantly greater in mice that received citrullinated ENA-78/CXCL5 compared with those that received PBS or noncitrullinated ENA-78/CXCL5 and were also significantly greater in mice that received noncitrullinated ENA-78/CXCL5 compared with those that received PBS. **B,** Left, Hematoxylin and eosin (H&E)–stained mouse knee joint sections, showing inflammatory cell infiltration in all groups and severe inflammation in mice treated with citrullinated ENA-78/CXCL5. Right, Immunofluorescence-stained mouse knee joint sections, showing a greater number of F4/80-positive monocyte/macrophages in mice treated with citrullinated ENA-78/CXCL5. Fluorescent red and blue staining show F4/80-positive monocyte/macrophages and cell nuclei, respectively. Original magnification × 400. **C,** Numbers of F4/80-positive monocyte/macrophages in mice treated with PBS, noncitrullinated ENA-78/CXCL5, and citrullinated ENA-78/CXCL5. Values are the mean ± SEM (n values are the number of joints). See Figure 4 for other definitions.

injected PBS, noncitrullinated ENA-78/CXCL5, or citrullinated ENA-78/CXCL5 into mouse knee joints. Joints injected with citrullinated ENA-78/CXCL5 had a significantly greater increase in circumference (mean ± SEM 3.0 ± 0.3 mm), and hence joint swelling, compared with knees injected with PBS (0.4 ± 0.2 mm; $P < 0.05$) or noncitrullinated ENA-78/CXCL5 (1.7 ± 0.3 mm; $P < 0.05$). Joints injected with noncitrullinated ENA-78/CXCL5 had significantly increased joint swelling compared with joints injected with PBS ($P < 0.05$) (Figure 5A). H&E staining showed inflammatory cell infiltration in each treatment group, and inflammation was especially severe in the group that received citrullinated ENA-78/CXCL5 (Figure 5B). Immunofluorescence staining revealed that the number of F4/80-positive monocyte/macrophages was significantly higher in mouse knee joints injected with citrullinated ENA-78/CXCL5 (mean ± SEM 67 ± 7 macrophages) compared with joints injected with noncitrullinated ENA-78/CXCL5 (40 ± 3 macrophages) or PBS (21 ± 4 macrophages). In addition, the number of F4/80-positive monocyte/macrophages was significantly higher in the mice treated with noncitrullinated ENA-78/CXCL5 compared with those that received PBS ($P < 0.05$) (Figures 5B and C).

DISCUSSION

We observed the presence of citrullinated ENA-78/CXCL5, MIP-1α/CCL3, and MCP-1/CCL2 in RA sera and RA SF. There is evidence that some chemokines can be citrullinated in vitro (27–30); however, not all cytokines can be citrullinated. Proost et al showed that PAD efficiently and site-specifically citrullinated ENA-78/CXCL5 and IL-8/CXCL8 but not IL-1β (27). Struyf et al demonstrated that stromal cell–derived factor 1 (SDF-1)/CXCL12 can be citrullinated in vitro, and that SDF-1/CXCL12 and PAD were coexpressed in

the colon tissue of patients with Crohn's disease (30). However, those investigators did not directly demonstrate the presence of citrullinated SDF-1/CXCL12 in diseased colon tissue.

In the current study, we demonstrated that the concentrations of citrullinated ENA-78/CXCL5, MIP-1α/CCL3, and MCP-1/CCL2 were all significantly higher in RA sera than in normal control sera. Furthermore, citrullinated ENA-78/CXCL5 and MIP-1α/CCL3 concentrations were significantly higher in RA SF than in SF from patients with OA and patients with other rheumatic diseases, and the level of citrullinated MCP-1/CCL2 was significantly higher in RA SF than in OA SF. In particular, the concentration of citrullinated ENA-78/CXCL5 was high in RA SF but was barely detected in SF from patients with OA or other rheumatic diseases. Additionally, the PAD4 level measured by ELISA is significantly elevated in RA SF compared with SF from patients with OA and patients with ankylosing spondylitis (31). This fact supports the notion that chemokines, including ENA-78/CXCL5, are citrullinated more efficiently in RA joints than in the inflamed joints of patients with other diseases. In our study, the concentrations of ENA-78/CXCL5 and MIP-1α/CCL3 in SF as measured by standard ELISA kits (R&D Systems) were lower than the concentrations of citrullinated ENA-78/CXCL5 and MIP-1α/CCL3 in SF as measured by the new ELISA system developed by our group. We observed that after citrullination, purified chemokines were not detected by standard ELISAs (data not shown). It is possible that these ELISAs may not completely recognize citrullinated chemokines in RA SF.

We showed that among 3 citrullinated chemokines tested in RA SF, the concentrations of citrullinated ENA-78/CXCL5 correlated most closely with clinical data (the CRP level and the ESR). Chemokines are readily detectable in RA SF (11,32–36), and the concentrations of MIP-1α/CCL3 and IL-8/CXCL8 in SF correlate with CRP levels in serum (35,36). In our study, we observed significant positive correlations between citrullinated ENA-78/CXCL5 and not only the CRP level but also the ESR, whereas the ENA-78/CXCL5 concentration did not correlate with any clinical parameters examined (data not shown). These results suggest that compared with the other chemokines that we examined, citrullinated ENA-78/CXCL5 is more closely related to disease activity in RA.

Citrullination has been reported to decrease the activities of certain chemokines in some instances (37). In vitro, ENA-78/CXCL5 (0.1–10 n*M*) induces PMN migration in a dose-responsive manner (10,25). However, citrullination of ENA-78/CXCL5 has been reported to reduce in vitro and in vivo PMN chemotaxis, intracellular calcium signaling, phosphorylation of extracellular signal–regulated kinase, and internalization of CXCR2 compared with noncitrullinated ENA-78/CXCL5 (38). We showed that citrullination of ENA-78/CXCL5 directly supports monocyte migration but not PMN migration. These results indicate the possibility that citrullination of ENA-78/CXCL5 does not increase the function of ENA-78/CXCL5 as a PMN recruiter but instead dampens it.

Surprisingly, we observed that citrullinated ENA-78/CXCL5 acquired a monocyte-recruiting function that noncitrullinated ENA-78/CXCL5 did not have. Normally, ENA-78/CXCL5 is not a potent chemotactic factor for monocytes but rather for PMNs and endothelial cells and also possesses angiogenic properties (10,25,39,40). Monocyte chemotaxis assays showed that citrullinated ENA-78/CXCL5 recruited monocytes in a dose-dependent manner, while noncitrullinated ENA-78/CXCL5 did not. These results suggest that citrullination of ENA-78/CXCL5 results in its conversion from a non–monocyte-recruiting chemokine to a monocyte-recruiting chemokine.

We then investigated whether citrullinated ENA-78/CXCL5 recruited monocytes through the G protein–coupled receptors CXCR2, which is the primary ENA-78/CXCL5 receptor, and CXCR1, which has 78% homology with CXCR2 at the amino acid level (41,42). Citrullinated ENA-78–induced monocyte migration was completely inhibited by pertussis toxin (a G protein–coupled receptor antagonist) or by a combination of anti-CXCR1 and anti-CXCR2 antibodies. These results suggest that citrullinated ENA-78/CXCL5 recruits monocytes via both CXCR1 and CXCR2. ENA-78/CXCL5 elicits PMN chemotaxis by interacting with the chemokine receptor CXCR2 present on the PMN cell surface (43,44). This receptor is expressed on many different cells including PMNs and monocytes (45). CXCR1 is also present on the surface of human monocytes (26,46). CXCR1 and CXCR2 are expressed on 23–90% and 22–93% of human monocytes, respectively (26). IL-8/CXCL8, neutrophil-activating peptide/CXCL7, growth-related oncogene α/CXCL1, and ENA-78/CXCL5 bind to CXCR2 with high affinity, whereas IL-8/CXCL8 exhibits high affinity for CXCR1 as well (47,48). Our results suggest that citrullination may increase the affinity of ENA-78/CXCL5 for CXCR1 (38).

We clearly show that at physiologically relevant concentrations, citrullinated ENA-78/CXCL5 recruits

monocytes. We also show data confirming that citrullinated ENA-78/CXCL5 preferentially binds to the CXCR1 receptor instead of the normal receptor for ENA-78/CXCL5, namely CXCR2. This indicates that modification of ENA-78/CXCL5 changes its receptor-binding affinity (and likely its conformation). This also explains, at least in part, the ability of citrullinated ENA-78/CXCL5 to recruit monocytes. Nonetheless, assuming that both citrullinated ENA-78/CXCL5 and noncitrullinated ENA-78/CXCL5 are present in SF and are binding to the same receptor, the modified or unmodified forms of ENA-78/CXCL5 that are present in greater quantities would be the forms that are more competitive for binding the available receptor. However, we now present evidence that citrullinated ENA-78/CXCL5 utilizes an alternative receptor (CXCR1), indicating that the concentration of citrullinated ENA-78/CXCL5 is likely more important when considering the monocyte-recruiting activity of citrullinated ENA-78/CXCL5. We believe that the conversion of ENA-78/CXCL5, a potent neutrophil recruitment factor to citrullinated ENA-78/CXCL5, an active monocyte recruitment factor, represents a change to a more chronic inflammatory response in RA-affected joints.

Last, we examined whether citrullination of ENA-78/CXCL5 results in increased inflammation and monocyte migration in vivo compared with noncitrullinated ENA-78/CXCL5. To test this hypothesis, we injected noncitrullinated or citrullinated ENA-78/CXCL5 into mouse knee joints and evaluated joint inflammation and monocyte migration. Citrullinated ENA-78/CXCL5 increased the knee circumference more than noncitrullinated ENA-78/CXCL5. Immunofluorescence staining showed that citrullinated ENA-78/CXCL5 induced more F4/80-positive monocyte/macrophage ingress into the synovial tissue of mouse knees compared with noncitrullinated ENA-78/CXCL5. These results suggest that citrullination of ENA-78/CXCL5 induces more severe inflammation in mouse knee joints through monocyte recruitment.

In the current study, although RA sera and RA SF were obtained from different groups of patients, the concentration of citrullinated ENA-78/CXCL5 in RA SF was higher than that in RA sera. These results suggest that citrullinated ENA-78/CXCL5 may be produced mainly in the joints and functions to recruit monocytes to the joints. Other citrullinated proteins (e.g, citrullinated vimentin) stimulate proinflammatoy cytokine production from fibroblast-like synoviocytes or peripheral blood mononuclear cells in RA (49,50). It is possible that citrullinated ENA-78/CXCL5 may also stimulate cells other than monocytes in mouse knee joints to release inflammatory mediators and aggravate the inflammatory response.

In addition, our study demonstrated that noncitrullinated ENA-78/CXCL5 recruited more monocyte/macrophages in vivo compared with PBS. In general, ENA-78/CXCL5 recruits neutrophils in vitro and in vivo. However, it is possible that other types of cells besides neutrophils respond to ENA-78/CXCL5 in vivo. It has been reported that macrophages, which are either inflammatory monocyte-derived cells or reemerging tissue-resident macrophages, increase in number during acute inflammatory responses (51). It is quite possible that the number of monocyte/macrophages increases in vivo during ENA-78/CXCL5–induced acute inflammation.

In conclusion, citrullinated ENA-78/CXCL5 was detected in RA SF and sera. The concentrations were significantly higher in SF from patients with RA than in SF from patients with OA or other inflammatory rheumatic diseases and correlated with the CRP level and the ESR. Citrullinated ENA-78/CXCL5 induced monocyte migration via CXCR1 and CXCR2 in vitro, while noncitrullinated ENA-78/CXCL5 did not. Mouse knees injected with citrullinated ENA-78/CXCL5 had more inflammation and monocyte/macrophages than did those injected with noncitrullinated ENA-78/CXCL5, suggesting that citrullination enhances the proinflammatory activity of ENA-78/CXCL5 and accelerates disease progression in inflammatory arthritis.

ACKNOWLEDGMENTS

We thank Dr. David A. Fox (Division of Rheumatology, University of Michigan Medical School) for helpful comments and interpretation of the results; Dr. Henriette A. Remmer (Proteomics & Peptide Synthesis Core, University of Michigan Medical School) and Dr. Michael Ford (MS Bioworks) for helpful comments on the mass spectrometry data and for providing the spectra; and Ray A. Ohara (University of Michigan) for assistance performing the experiments.

AUTHOR CONTRIBUTIONS

All authors were involved in drafting the article or revising it critically for important intellectual content, and all authors approved the final version to be published. Dr. Yoshida had full access to all of the data in the study and takes responsibility for the integrity of the data and the accuracy of the data analysis.

Study conception and design. Yoshida, Korchynskyi, Tak, Ruth, Campbell, Amin, Koch.

Acquisition of data. Yoshida, Korchynskyi, Isozaki, Baeten, Gerlag, Amin.

Analysis and interpretation of data. Yoshida, Korchynskyi, Ruth, Campbell, Koch.

REFERENCES

1. Tak PP, Bresnihan B. The pathogenesis and prevention of joint damage in rheumatoid arthritis: advances from synovial biopsy and tissue analysis. Arthritis Rheum 2000;43:2619–33.
2. Van Venrooij WJ, van Beers JJ, Pruijn GJ. Anti-CCP antibodies: the past, the present and the future. Nat Rev Rheumatol 2011;7: 391–8.
3. Schellekens GA, de Jong BA, van den Hoogen FH, van de Putte LB, van Venrooij WJ. Citrulline is an essential constituent of antigenic determinants recognized by rheumatoid arthritis-specific autoantibodies. J Clin Invest 1998;101:273–81.
4. Sebbag M, Moinard N, Auger I, Clavel C, Arnaud J, Nogueira L, et al. Epitopes of human fibrin recognized by the rheumatoid arthritis-specific autoantibodies to citrullinated proteins. Eur J Immunol 2006;36:2250–63.
5. Suzuki A, Yamada R, Yamamoto K. Citrullination by peptidylarginine deiminase in rheumatoid arthritis. Ann N Y Acad Sci 2007;1108:323–39.
6. Mangat P, Wegner N, Venables PJ, Potempa J. Bacterial and human peptidylarginine deiminases: targets for inhibiting the autoimmune response in rheumatoid arthritis? Arthritis Res Ther 2010;12:209.
7. Szekanecz Z, Kim J, Koch AE. Chemokines and chemokine receptors in rheumatoid arthritis. Semin Immunol 2003;15:15–21.
8. Haringman JJ, Ludikhuize J, Tak PP. Chemokines in joint disease: the key to inflammation? Ann Rheum Dis 2004;63:1186–94.
9. Zlotnik A, Yoshie O. Chemokines: a new classification system and their role in immunity. Immunity 2000;12:121–7.
10. Walz A, Burgener R, Car B, Baggiolini M, Kunkel SL, Strieter RM. Structure and neutrophil-activating properties of a novel inflammatory peptide (ENA-78) with homology to interleukin 8. J Exp Med 1991;174:1355–62.
11. Koch AE, Kunkel SL, Harlow LA, Mazarakis DD, Haines GK, Burdick MD, et al. Epithelial neutrophil activating peptide-78: a novel chemotactic cytokine for neutrophils in arthritis. J Clin Invest 1994;94:1012–8.
12. Halloran MM, Woods JM, Strieter RM, Szekanecz Z, Volin MV, Hosaka S, et al. The role of an epithelial neutrophil-activating peptide-78-like protein in rat adjuvant-induced arthritis. J Immunol 1999;162:7492–500.
13. Kinloch A, Tatzer V, Wait R, Peston D, Lundberg K, Donatien P, et al. Identification of citrullinated α-enolase as a candidate autoantigen in rheumatoid arthritis. Arthritis Res Ther 2005;7: R1421–9.
14. Van Steendam K, Tilleman K, De Ceuleneer M, De Keyser F, Elewaut D, Deforce D. Citrullinated vimentin as an important antigen in immune complexes from synovial fluid of rheumatoid arthritis patients with antibodies against citrullinated proteins. Arthritis Res Ther 2010;12:R132.
15. Vossenaar ER, Smeets TJ, Kraan MC, Raats JM, van Venrooij WJ, Tak PP. The presence of citrullinated proteins is not specific for rheumatoid synovial tissue. Arthritis Rheum 2004;50:3485–94.
16. Foulquier C, Sebbag M, Clavel C, Chapuy-Regaud S, Al Badine R, Mechin MC, et al. Peptidyl arginine deiminase type 2 (PAD-2) and PAD-4 but not PAD-1, PAD-3, and PAD-6 are expressed in rheumatoid arthritis synovium in close association with tissue inflammation. Arthritis Rheum 2007;56:3541–53.
17. Korchynskyi O, ten Dijke P. Identification and functional characterization of distinct critically important bone morphogenetic protein-specific response elements in the Id1 promoter. J Biol Chem 2002;277:4883–91.
18. Senshu T, Sato T, Inoue T, Akiyama K, Asaga H. Detection of citrulline residues in deiminated proteins on polyvinylidene difluoride membrane. Anal Biochem 1992;203:94–100.
19. Tsuji Y, Akiyama M, Arita K, Senshu T, Shimizu H. Changing pattern of deiminated proteins in developing human epidermis. J Invest Dermatol 2003;120:817–22.
20. Kubota K, Yoneyama-Takazawa T, Ichikawa K. Determination of sites citrullinated by peptidylarginine deiminase using 18O stable isotope labeling and mass spectrometry. Rapid Commun Mass Spectrom 2005;19:683–8.
21. Ruth JH, Haas CS, Park CC, Amin MA, Martinez RJ, Haines GK III, et al. CXCL16-mediated cell recruitment to rheumatoid arthritis synovial tissue and murine lymph nodes is dependent upon the MAPK pathway. Arthritis Rheum 2006;54:765–78.
22. Ruth JH, Arendt MD, Amin MA, Ahmed S, Marotte H, Rabquer BJ, et al. Expression and function of CXCL16 in a novel model of gout. Arthritis Rheum 2010;62:2536–44.
23. Koch AE, Burrows JC, Marder R, Domer PH, Leibovich SJ. Reactivity of human tissues with monoclonal antibodies to myeloid activation and differentiation antigens: an immunohistochemical study. Pathobiology 1990;58:241–8.
24. Prevoo ML, van 't Hof MA, Kuper HH, van Leeuwen MA, van de Putte LB, van Riel PL. Modified disease activity scores that include twenty-eight–joint counts: development and validation in a prospective longitudinal study of patients with rheumatoid arthritis. Arthritis Rheum 1995;38:44–8.
25. Wuyts A, Govaerts C, Struyf S, Lenaerts JP, Put W, Conings R, et al. Isolation of the CXC chemokines ENA-78, GRO α and GRO γ from tumor cells and leukocytes reveals NH2-terminal heterogeneity: functional comparison of different natural isoforms. Eur J Biochem 1999;260:421–9.
26. Gerszten RE, Garcia-Zepeda EA, Lim YC, Yoshida M, Ding HA, Gimbrone MA, et al. MCP-1 and IL-8 trigger firm adhesion of monocytes to vascular endothelium under flow conditions. Nature 1999;398:718–23.
27. Proost P, Loos T, Mortier A, Schutyser E, Gouwy M, Noppen S, et al. Citrullination of CXCL8 by peptidylarginine deiminase alters receptor usage, prevents proteolysis, and dampens tissue inflammation. J Exp Med 2008;205:2085–97.
28. Loos T, Opdenakker G, Van Damme J, Proost P. Citrullination of CXCL8 increases this chemokine's ability to mobilize neutrophils into the blood circulation. Haematologica 2009;94:1346–53.
29. Loos T, Mortier A, Gouwy M, Ronsse I, Put W, Lenaerts JP, et al. Citrullination of CXCL10 and CXCL11 by peptidylarginine deiminase: a naturally occurring posttranslational modification of chemokines and new dimension of immunoregulation. Blood 2008;112:2648–56.
30. Struyf S, Noppen S, Loos T, Mortier A, Gouwy M, Verbeke H, et al. Citrullination of CXCL12 differentially reduces CXCR4 and CXCR7 binding with loss of inflammatory and anti-HIV-1 activity via CXCR4. J Immunol 2009;182:666–74.
31. Chang X, Zhao Y, Sun S, Zhang Y, Zhu Y. The expression of PADI4 in synovium of rheumatoid arthritis. Rheumatol Int 2009; 29:1411–6.
32. Koch AE, Kunkel SL, Harlow LA, Johnson B, Evanoff HL, Haines GK, et al. Enhanced production of monocyte chemoattractant protein-1 in rheumatoid arthritis. J Clin Invest 1992;90:772–9.
33. Koch AE, Kunkel SL, Harlow LA, Mazarakis DD, Haines GK, Burdick MD, et al. Macrophage inflammatory protein-1 α: a novel chemotactic cytokine for macrophages in rheumatoid arthritis. J Clin Invest 1994;93:921–8.
34. Akahoshi T, Wada C, Endo H, Hirota K, Hosaka S, Takagishi K, et al. Expression of monocyte chemotactic and activating factor in rheumatoid arthritis: regulation of its production in synovial cells by interleukin-1 and tumor necrosis factor. Arthritis Rheum 1993;36:762–71.
35. Hatano Y, Kasama T, Iwabuchi H, Hanaoka R, Takeuchi HT, Jing L, et al. Macrophage inflammatory protein 1 α expression by synovial fluid neutrophils in rheumatoid arthritis. Ann Rheum Dis 1999;58:297–302.
36. Peichl P, Ceska M, Effenberger F, Haberhauer G, Broell H,

Lindley IJ. Presence of NAP-1/IL-8 in synovial fluids indicates a possible pathogenic role in rheumatoid arthritis. Scand J Immunol 1991;34:333–9.
37. Mortier A, Gouwy M, Van Damme J, Proost P. Effect of post-translational processing on the in vitro and in vivo activity of chemokines. Exp Cell Res 2011;317:642–54.
38. Mortier A, Loos T, Gouwy M, Ronsse I, Van Damme J, Proost P. Posttranslational modification of the NH2-terminal region of CXCL5 by proteases or peptidylarginine deiminases (PAD) differently affects its biological activity. J Biol Chem 2010;285: 29750–9.
39. Strieter RM, Polverini PJ, Kunkel SL, Arenberg DA, Burdick MD, Kasper J, et al. The functional role of the ELR motif in CXC chemokine-mediated angiogenesis. J Biol Chem 1995;270: 27348–57.
40. Koch AE, Volin MV, Woods JM, Kunkel SL, Connors MA, Harlow LA, et al. Regulation of angiogenesis by the C-X-C chemokines interleukin-8 and epithelial neutrophil activating peptide 78 in the rheumatoid joint. Arthritis Rheum 2001;44:31–40.
41. Holmes WE, Lee J, Kuang WJ, Rice GC, Wood WI. Structure and functional expression of a human interleukin-8 receptor. Science 1991;253:1278–80.
42. Murphy PM, Tiffany HL. Cloning of complementary DNA encoding a functional human interleukin-8 receptor. Science 1991;253: 1280–3.
43. Persson T, Monsef N, Andersson P, Bjartell A, Malm J, Calafat J, et al. Expression of the neutrophil-activating CXC chemokine ENA-78/CXCL5 by human eosinophils. Clin Exp Allergy 2003;33: 531–7.
44. Horuk R. Chemokine receptors. Cytokine Growth Factor Rev 2001;12:313–35.
45. Chapman RW, Phillips JE, Hipkin RW, Curran AK, Lundell D, Fine JS. CXCR2 antagonists for the treatment of pulmonary disease. Pharmacol Ther 2009;121:55–68.
46. Browning DD, Diehl WC, Hsu MH, Schraufstatter IU, Ye RD. Autocrine regulation of interleukin-8 production in human monocytes. Am J Physiol Lung Cell Mol Physiol 2000;279:L1129–36.
47. Ludwig A, Petersen F, Zahn S, Gotze O, Schroder JM, Flad HD, et al. The CXC-chemokine neutrophil-activating peptide-2 induces two distinct optima of neutrophil chemotaxis by differential interaction with interleukin-8 receptors CXCR-1 and CXCR-2. Blood 1997;90:4588–97.
48. Murphy PM, Baggiolini M, Charo IF, Hebert CA, Horuk R, Matsushima K, et al. International union of pharmacology. XXII. Nomenclature for chemokine receptors. Pharmacol Rev 2000;52: 145–76.
49. Snir O, Rieck M, Gebe JA, Yue BB, Rawlings CA, Nepom G, et al. Identification and functional characterization of T cells reactive to citrullinated vimentin in HLA–DRB1*0401–positive humanized mice and rheumatoid arthritis patients. Arthritis Rheum 2011;63: 2873–83.
50. Fan LY, He DY, Wang Q, Zong M, Zhang H, Yang L, et al. Citrullinated vimentin stimulates proliferation, pro-inflammatory cytokine secretion, and PADI4 and RANKL expression of fibroblast-like synoviocytes in rheumatoid arthritis. Scand J Rheumatol 2012;41:354–8.
51. Liddiard K, Rosas M, Davies LC, Jones SA, Taylor PR. Macrophage heterogeneity and acute inflammation. Eur J Immunol 2011;41:2503–8.

2015

University of Michigan
Hospital and Health
Systems

Gautam Edhayan

Running Title: Id1 as a fibroblast derived inflammatory agonist in RA

Inflammatory Properties of Inhibitor of DNA Binding 1 as a Unique Fibroblast Derived Nuclear Protein

Gautam Edhayan[1], Christine M. Ha[1], Takeo Isozaki[1], M. Asif Amin[1], Ray A. Ohara[1], Rachel Morgan[1], Phillip L. Campbell[1], G. Kenneth Haines III[2], Ali S. Arbab[3], Sean C. Friday[1], W. Alex Stinson[1], David A. Fox[1], and Jeffrey H. Ruth[1]

[1]University of Michigan Medical School, Ann Arbor, MI 48109; [2]Mount Sinai Health System, New York, NY 10019, [3]Henry Ford Hospital & Medical Centers, Detroit, MI 48202

This work was supported by a grant from the Department of Defense (PR120641). Additional support included the Frederick G.L. Huetwell and William D. Robinson, M.D. Professorship in Rheumatology.

Correspondence address: Jeffrey H. Ruth, Ph.D.
University of Michigan Medical School
Department of Medicine, Division of Rheumatology
109 Zina Pitcher Drive, 4023 BSRB
Ann Arbor, MI 48109-2200
Phone: 734-615-9374; Fax: 734-615-2506
Email: jhruth@med.umich.edu

Conflicts of interest: none

Keywords: Inhibitor of DNA binding-1 protein, inflammation, rheumatoid arthritis, fibroblasts.

Abstract

Background: Inhibitor of DNA binding 1 (Id1) is a nuclear protein containing a basic helix-loop-helix (bHLH) domain that regulates cell growth by selective binding and prevention of gene transcription.

Methods: Histologic analysis correlated cellular expression of Id1 with inflammatory scores in rheumatoid arthritis synovial tissue (RA ST) and K/BxN serum induced mouse joints. Fibroblast supernatants subjected to differential centrifugation to isolate and purify exosomes were measured for Id1 by enzyme linked immunosorbant assay (ELISA). For signal transduction analysis, Western blots were done on Id1 stimulated endothelial cells (ECs) to determine the kinetics of intracellular protein phosphorylation. EC intracellular signaling pathways induced by Id1 were subsequently targeted with silencing RNA (siRNA) for angiogenesis inhibition.

Results: Lining cells produce Id1 in STs and correlated with inflammatory scores in human RA ST and joints from K/BxN serum induced mice. Normal (NL) and RA synovial fibroblasts increased Id1 production with stimulation by transforming growth factor- β (TGF-β). We found that >80% of the Id1 released by RA synovial fibroblasts is contained within exosomes. Endothelial progenitor cells (EPCs) and human dermal microvascular ECs (HMVECs) share the Jnk signaling pathway in response to Id1. Finally, we show that Jnk siRNA reverses Id1 induced HMVEC vessel formation in Matrigel plugs in vivo.

Conclusion: Id1 is a pleotropic molecule affecting angiogenesis, vasculogenesis, and fibrosis. Our data shows that Id1 is not only an important nuclear protein, but also that it can be released from fibroblasts via exosomes, thus expanding its role in the orchestration of inflammatory lesions.

Introduction

Rheumatoid arthritis (RA) is a systemic autoimmune disease characterized by inflammation and joint destruction. Angiogenesis is important in a variety of vasculoproliferative states such as wound repair and chronic inflammation seen in RA. Many inflammatory mediators found in RA synovial tissues (STs) and synovial fluids (SFs) display angiogenic properties. Id1 is a member of the helix-loop-helix (HLH) family of transcription factors and a marker of cellular self-renewal. Inhibition of Id1 in the bone marrow (BM) results in significant decreases in EPC linked tumor associated vasculogenesis (1). Id1 lacks DNA binding activity, but does form heterodimers with members of the bHLH family of transcription factors allowing Id1 to inhibit DNA binding and transcriptional activation of proteins with which it interacts. bHLH proteins such as BMAL1-Clock (*Circadian Locomotor Output Cycles Kaput*) (2), which is a core transcription complex in the molecular circadian clock binds Id1. Id1 also interacts with other genes, like c-Myc (3) and hypoxia-inducible factor-1 (HIF-1) (4), that have been linked to cancer due to their effects on cell growth and metabolism. Id1 also binds tightly with ubiquitously expressed E proteins. E proteins heterodimerize with tissue restricted bHLH proteins to form active transcription complexes, so by sequestering E proteins, Id1 inhibits tissue restricted gene expression in multiple cell lineages using the same biochemical mechanism (5, 6).

The human Id1 gene has been cloned and characterized by Hara et al (7), who also cloned a related gene, Id2. Although a splice variant (Id1-prime) that does not show the growth regulated expression normally seen with Id1 has also been described (8), Id1 is related to Id2 and Id3 (9). Id1 and Id3 have been identified as negative regulators of pluripotent stem cell maturation (10), and supports the view that Id1 is highly characteristic of progenitor cells and/or cells that exhibit hyperproliferative responses. As a protein affecting the activity of many transcription factors, Id1 can affect multiple cellular properties. Targeting EPCs by way of Id1 transcription blocks EPC mobilization, causes angiogenesis inhibition,

impairs the spread of metastasis, and increases the survival of tumor bearing mice (1, 11). Human Id1 mRNA is barely detectable in quiescent early passage fibroblasts, but its expression can be induced by serum. Interestingly, Id1 antisense RNA prevents early passage fibroblasts from entering the S phase of the cell cycle (7).

Histologic analysis of ST revealed that Id1 is highly expressed in the vasculature of RA ST (12), and on synovial lining cells (pre-fibroblast/monocyte), suggesting that Id1 displays pleiotropic properties in pre-mature phenotypic cells found in the RA synovium. This indicates that Id1 expressing cells located in blood vessels lining the RA synovium are likely bone marrow (BM) derived (12), and in agreement with the findings of Sakurai et al, who showed substantial expression of Id1 and Id3 in RA compared to osteoarthritis (OA) synovium at the protein and transcriptional levels (13). Gao et al subsequently showed that it was possible to identify, track, and target BM derived endothelial progenitor cells (EPCs) in vivo using a mouse model of pulmonary metastasis by way of Id1 expression (1, 11). Our group was the first to report that RA synovial fluid (SF) contains abundant amounts of Id1 and we now show that the primary sources are from activated RA fibroblasts. We also found that Id1 is packaged within extracellular vesicles (EVs) and released from fibroblasts via exosomes. Once released, Id1 induces signaling pathways in ECs inducing angiogenic responses (12), that can be targeted to reduce blood vessel growth. Overall, our data is suggestive that fibroblast derived Id1 may contribute to vasculogenesis as well as angiogenesis by independent mechanisms, and that soluble Id1 can serve as either a biomarker or therapeutic target for angiogenesis in RA tissues.

Materials and Methods

Ethical use of animals: The University of Michigan's Unit for Laboratory Animal Medicine (ULAM) is an AAALAC (Association for Assessment and Accreditation of Laboratory Animal Care) accredited facility. Treatment of animals in this study was approved by ethics

committees at the University of Michigan. ULAM is supervised by a veterinarian and operates in accordance with federal regulations. Mice were housed in sterile rodent micro-isolator caging with filtered cage tops in a specific pathogen-free environment to prevent infection. Severe combined immunodeficiency (SCID) mice were obtained from National Cancer Institute (NCI). C57/BL6 wildtype (Wt) mice were bred in house according to the guidelines of the University Committee on the Use and Care of Animals. All efforts were made to reduce stress or discomfort in the animals used in these studies.

K/BxN serum induced arthritis model: To generate arthritic K/BxN mice, K/B positive mice were crossed with NOD/LTj mice as previously described (14). Naïve mice at the age of 5-7 weeks were injected with 150 µL of K/BxN serum intraperitoneally, and this was considered day 0 of arthritis. Another injection of 150 µL of K/BxN serum followed on day 2. Robust arthritis with severe swelling of the joints typically developed on day 5. Articular index (AI) scores and joint circumferences were determined starting on day 0 and scored at least every other day up to day 23 after arthritis induction of arthritis as described previously for rat adjuvant induced arthritis (15). Clinical scoring for arthritis was performed using a 0–4 AI scale, where 0 = no swelling or erythema, 1 = slight swelling and/or erythema, 2 = low-to-moderate edema, 3 = pronounced edema with limited use of the joint, and 4 = excessive edema with joint rigidity. All measurements were taken by observers blinded to the experimental conditions. Mouse ankles were harvested for histology.

Immunohistochemisty (IHC): RA, OA, and NL (not arthritis) ST cryo-sections as well as ankle sections of Wt mice induced with K/BxN serum were fixed in cold acetone for 30 minutes at 4°C. The tissue sections were blocked with 5% donkey serum and 20% FBS in phosphate-buffered saline (PBS) at 37°C for 1 hour. The sections were then incubated with either mouse anti-human Id1 antibody (Abcam, Cambridge, United Kingdom, 10 µg/mL), rabbit anti-mouse

Id1 antibody (CalBioreagents, San Mateo, USA, 10 μg/mL), or purified nonspecific mouse and rabbit IgG (Thermo) for 1 hour at 37°C in blocking buffer. After washing, tissues were incubated with a biotinylated anti-mouse or anti-rabbit secondary antibody (Vector Labs, Burlingame, USA, 10 μg/mL) for 1 hour at 37°C in blocking buffer. Vectastain ABC kit (Vector Labs) was used to detect the antibodies on the tissues, all manufacturer protocols were followed. Sections were mounted with Cytoseal 60 (Thermo). Sections were visualized under a microscope (Olympus, Tokyo, Japan) and were scored by a pathologist.

Cell Culture: EPCs were collected from Henry Ford Hospital. HMVECs as well as all fibroblasts were collected from human tissues which were digested in a mix of cell culture media supplemented with fetal bovine serum (FBS), collagenase, and hyaluronidase. HMVECs were isolated from skin biopsies while the fibroblasts were isolated from synovial tissues of patients with their diagnosed disease. HMVECs were isolated and purified using CD31 microbeads (Miltenyi Biotec, Bergisch Gladbach, Germany). HMVECs were grown in EBM-2 (Lonza, Basel, Switzerland) and were placed in reduced serum EBM-1 before stimulation. EBM-1 without serum was used for HMVEC stimulations. EPCs were grown and stimulated in StemSpan SFEM (Stemcell Technologies, Vancouver, Canada) with no added supplement. Fibroblasts were grown in RPMI-1640 (Thermo, Waltham, USA) supplemented with 10% FBS and were stimulated in serum free RPMI-1640.

Enzyme-Linked Immunosorbent Assay (ELISA): HMVECs, EPCs, monocytes, and RA, OA, and NL synovial fibroblasts were plated in 6-well plates at 200,000 cells/well and serum starved overnight. Media was exchanged and collected after 24 hours. The collected media was analyzed by ELISA for Id1 (MyBioSource, San Diego, USA). Manufacturer protocols were followed. SFs of RA, OA, and several other diseases were also analyzed by this ELISA. Both synovial and dermal fibroblasts were stimulated with varying cytokines and

concentrations. Cytokines used were Tumor necrosis factor alpha (TNFα, Life Technologies, Carlsbad, USA), Chemokine (C-X-C motif) ligand 16 (CXCL16, R&D Systems, Minneapolis, USA), Interleukin 17 (IL-17, R&D Systems), and TGF-β (R&D Systems). These cytokines were chosen because they are known to be upregulated and involved in the pathogenesis of RA and other fibrotic diseases (16, 17). The supernatant after 24 hours stimulation was collected and analyzed by this ELISA. The exosome fractions were also analyzed by this ELISA.

Exosome Purification: Exosomes were isolated from cell culture supernatants with differential centrifugation. RA synovial fibroblasts were plated at 200,000 cells/well in a 6-well tissue culture plate in serum free media. Media was exchanged and incubated for 24-hours after which the supernatant was collected. An aliquot of the supernatant was taken for later analysis and the remaining amount was subjected to several steps of differential centrifugation. All centrifugation was conducted at 4°C. First, the supernatant was centrifuged at 300 x g for 10 minutes to remove free cells. The remaining supernatant was centrifuged 10,000 x g to remove cellular debris. The remaining supernatant was centrifuged at 30,000 x g to remove smaller debris. The supernatant was then transferred to an ultra-centrifuge and spun at 110,000 x g overnight to pellet the exosomes. The supernatant was stored and the pellet was separated on an Optiprep density gradient (Sigma, St. Louis, USA). The fractions containing exosomes were then isolated. The original whole supernatant, exosome and cellular debris depleted fraction, exosome fraction, and exosome fraction lysed with 0.5% Triton X-100 (Sigma) were run on the Id1 ELISA.

Western Blotting: HMVECs or EPCs were plated in 6-well plates at 500,000 cells/well and serum starved overnight. The wells were then stimulated with Id1 (Abnova, Taipei, Taiwan, 10 nM) over a 45 minute time course. Cell lysates were prepared in reducing conditions and

western blot analysis was done. Proteins were transferred from the gel to nitrocellulose membranes which were then blocked in 5% nonfat dry milk in Tris-Buffered Saline + Tween-20 (TBST, pH 7.6). Membranes were probed with rabbit anti-human signaling antibodies to both the phosphorylated (*p) and non-phosphorylated forms of Jnk, $Erk_{1/2}$, PI3k, and P38 (Cell Signaling, Danvers, USA, 1:1000 dilution) in blocking buffer overnight at 4°C. Membranes were washed 3 times with TBST and incubated with horseradish peroxidase (HRP) conjugated donkey anti-rabbit antibody (Cell Signaling, 1:1000 dilution) for 1 hour at 25°C. Membranes were washed with TBST and visualized using Pierce ECL Western Blotting Substrate (Thermo). X-ray film was used to visualize the blots after ECL. These films were scanned and bands were quantified by UN-SCAN-IT (Silk Scientific, Orem, USA). Gel loading was accounted for by adjusting all phosphorylated data by the total amount of signaling protein, and fold change of the phosphorylated signal molecules was calculated with respect to the unstimulated lysate.

Severe Combined Immunodeficiency (SCID) Matrigel Plug Angiogensis Assay: To examine the effects of the Jnk pathway in angiogenesis with Id1 stimulation *in vivo*, SCID mice were injected subcutaneously with sterile Matrigel (BD Biosciences, 500 µL/injection) containing Id1 (10 nM) and Jnk silenced HMVECs. HMVECs were silenced using siRNA inhibiting the Jnk signaling molecule (Santa Cruz Biotechnology, Dallas, USA). Either Jnk siRNA or nonspecific siRNA was transfected into the HMVECs using the TransIT-TKO Transfection Reagent (Mirus Bio, Madison, USA). Manufacturer protocols were followed for the transfection. 24 hours after transfection, a portion of the cells were lysed to confirm Jnk knockdown and the rest were injected with the Matrigel ($2.5x10^5$ cells/injection). The Matrigel plugs were removed 5 days later and weighed. Hemoglobin (Hb) analysis was conducted on the plug homogenates as a measure of angiogenesis. Hb levels were measured by adding 25 µL of homogenate mixed with 25 µL of 3, 3′, 5, 5′-Tetramethylbenzidine (TMB) reagent to

96-well plates. Finally, samples were incubated at room temperature for 5 minutes. Absorbance was read with a microplate reader at 450nm. Hb concentration was determined by comparison with a standard curve in mg/mL. Hb concentration, after normalization with plug weight, is a reflection of the number of blood vessels in the tissue (18).

Results

Immunohistochemistry analysis of Id1 expression in mouse and human synovium: IHC staining for Id1 on RA, OA, and NL STs and K/BxN serum induced mouse ankles showed positive staining indicating the presence of Id1 in these tissues. Id1 is highly expressed on the vasculature and lining cells of RA ST as well as in the K/BxN serum induced mouse ankles (Figure 1). These images were taken at 400 x. Analysis of these tissues by a pathologist revealed that RA STs had a significantly higher percentage of lining cells positive for Id1 than OA and NL STs(Figure 2A). Similarly, the Day 12 K/BxN serum induced mouse ankles had more Id1 positive lining cells than Day 0 mouse ankles; however the difference is less in magnitude (Figure 2C). Correlating inflammatory score with the percentage of lining cells positive for Id1 showed a positive correlation in both RA and K/BxN serum induced mouse tissues (Figure B and D).

Determination of cytokine mediated fibroblast expression by ELISA: Analysis of supernatants of unstimulated cells of several types found in the RA synovium showed that synovial fibroblasts are the primary producer of Id1, and that RA fibroblasts produce more basal Id1 compared to NL and OA fibroblasts (Figure 3A). Monocytes also produce some Id1, however much less is produced when compared to synovial fibroblasts. The ECs produced an undetectable amount of Id1. ELISA analysis of NL synovial fibroblast cell culture supernatants stimulated with several different cytokines found Id1 concentration to be heightened with stimulation with certain cytokines. Results show that TGF-β (at 10 and 50

ng/mL) and to a lesser extent IL-17 (at 50 ng/mL) increase Id1 production in synovial fibroblasts (Figure 3B). TNF-α showed an initial increase in Id1 production at 10 ng/mL, then a slight decrease at 50 ng/mL when compared to the NS cells. CXCL16 showed the opposite trend with a slight decrease in Id1 production at 10 ng/mL, then a slight decrease at 50 ng/mL. ELISA analysis of RA, OA, and NL synovial fibroblast cell culture supernatants stimulated with TGF-β at 10 and 50 ng/mL showed that TGF-β has a large effect on Id1 production by synovial fibroblasts (Figure 3C). RA fibroblasts are significantly more sensitive to TGF- β stimulation with respect to Id1 production compared to OA and NL synovial fibroblasts. There is a slight decrease in Id1 production at 50 ng/mL of TGF-β in RA and NL fibroblasts when compared to Id1 production at 10 ng/mL. OA fibroblasts showed increasing amounts of Id1 production at both 10 and 50 ng/mL of TGF-β.

Identification of fibroblast exosomes by ELISA: Analysis of fractions taken during a successive series of steps to isolate exosomes using differential centrifugation from RA synovial cell supernatants showed that the majority of the Id1 is found within exosomes when compared to the other fractions (Figure 4). A small amount of Id1 is found in the whole supernatant and exosome depleted fractions, and no Id1 is found in the unlysed exosome fraction. Triton X-100 at 0.5% was used to lyse the exosomes and the majority of Id1 was found in this fraction.

Western blot analysis of Id1 mediated signaling in ECs: Western blot analysis of *pJnk in HMVECs and EPCs after a time course stimulation with Id1 shows that *pJnk is upregulated after 1 minute of stimulation with Id1 and continues upregulation at 45 minutes of stimulation in EPCs. However, in HMVECs upregulation was delayed by 15 minutes but continued to 45 minutes (Figures 5A and 5B). Analysis of *pP38 in EPCs showed that *pP38 is upregulated almost immediately after stimulation with Id1 and continues upregulation at 45 minutes of

stimulation (Figure 5C). *pErk and *pPI3k did not show any upregulation after Id1 stimulation in either EPCs or HMVECs and *pP38 did not show any upregulation in HMVECs after Id1 stimulation (Figure 5E). Data is shown as fold increase of phosphorylated signaling protein over the NS, after normalization with the total amount of signaling protein.

Matrigel plug angiogenesis assay: Hemoglobin analysis of the Matrigel (with HMVECs and 10 nM Id1) injected in the SCID mice showed less hemoglobin when the HMVECs were treated with Jnk siRNA when compared to the control siRNA (Figure 6). Hemoglobin concentration is representative of vascularization of the Matrigel plug. The results show that the Jnk siRNA significantly decreased the concentration of hemoglobin in Matrigel plugs.

Statistical analysis: Results are expressed as the mean ± SEM. Data were analyzed using a student's t-test. P values less than 0.05 were considered significant.

Discussion

Id1 is known to be a nuclear transcription factor characteristic of EPCs and cells that display a hyperproliferative phenotype. Our group has shown that Id1 is detected in RA synovium and SFs, and displays pro-angiogenic activity upon cell exit (12). Levels of Id1 are elevated in RA SFs and have been shown to correlate with expression of the angiogenic chemokine CXCL16 (the ligand for the CXCR6 receptor) (12). Correspondingly, CXCR6 knockout mice develop attenuated angiogenesis associated with profound decreases in arthritis progression and inflammatory cell recruitment to arthritic joints in K/BxN serum induced mice. We now present evidence that synovial fibroblasts are largely responsible for the elevated amounts of Id1 in RA SF, and that approximately 80% of the Id1 released by fibroblasts is packaged within exosomes. Finally, pro-inflammatory cytokines known to be elevated in RA patients such as IL-17 and especially TGF-β, induce significantly more

fibroblast derived Id1 in RA compared to OA or NL fibroblasts in vitro. Of special note, RA fibroblasts are significantly more sensitive to TGF-β stimulation than OA or NL fibroblasts with respect to Id1 production. This indicates that RA fibroblasts are different from NL or OA fibroblasts such that they can produce more Id1 in response to a pro-fibrotic stimulus. These findings indicate that RA fibroblasts are primed to release Id1 in response to pro-fibrotic and angiogenic mediators.

Histologic analysis of ST revealed that Id1 is highly expressed on synovial lining cells (pre-fibroblasts/monocytes) and in the vasculature of the RA ST (12) in complete agreement with Sakurai et al, who showed Id1 and Id3 mRNA and protein are elevated in RA synovium (13). We further show that lining cell expression of Id1 positively correlates with inflammatory scores in both the patient tissues and from joint tissues taken from K/BxN serum induced mice. Studies of knockout mice lacking expression of Id1 has shown its involvement in vasculogenesis and neuroblast differentiation in various cancer models normally characterized by extensive vascularization. Tumors transplanted into these mice failed to grow and metastasize due to lack of proper tumor angiogenesis. Branching and sprouting of blood vessels in the neuroectoderm is also defective in double knockout mice lacking expression of Id1 and the related Id3, as these animals show premature differentiation of neuroblasts (19). Thus it appears that Id1 expression is critical for angiogenic processes found in the tumor microenvironment or the RA joint, further suggesting that dysregulation of Id1 can lead to unwanted inflammatory outcomes. Furthermore, our findings provide additional evidence that Id1 may be used to assess or grade the severity of some pathologic conditions, as has been done for some cancers (20).

One of the many interesting features of Id1 is its ability to equally repress inhibitors of angiogenesis. Previous studies showed that Id1 indirectly regulates angiogenesis through transcriptional repression of thrombospondin-1 (21). The expression of diverse genes involved in remodeling of the extracellular matrix, angiogenesis and intracellular signaling are

also affected by Id1 (21). Furthermore, Id1 represses p21 (3) expression to control EPC growth and maturation in the BM. Because of the ability of Id1 to downregulate expression of these potent repressors, it was reported that Id1 can function as an effective pro-angiogenic mediator produced by EPCs and pluripotent stem cells (22). This idea was reinforced by reports identifying Id1 and Id3 as negative regulators of pluripotent stem cell maturation (10). Because of its potent regulatory control of angiogenic and vasculogenic processes, it was not surprising to find that Id1 acts as a negative transcriptional regulator for proteins associated with malignant melanoma development (23, 24).

It is well documented that Id1 is a regulatory nuclear protein, however, we and others have previously shown that Id1 can be detected on the ECs in the RA synovium and in soluble form in synovial effusions (12, 13). This suggests that Id1 travels outside the nucleus, but the functionality and method of this transfer has not been described. One thought is that Id1 may be packaged into EVs such as cellular exosomes that can be released into the joint space or directly into adjacent cells. To test this possibility, we isolated EVs from RA synovial fibroblast supernatants known to contain Id1, and measured Id1 in the EV and soluble protein fractions. We used differential ultracentrifugation to isolate EVs specifically around the size of exosomes. We visually confirmed a band at the density gradient between fractions 4 and 5 around where exosomes would be expected (density between 1.084 g/mL and 1.163 g/mL). To more clearly define where Id1 is located we further subdivided the EV fraction over a discontinuous Optiprep density gradient with seven fractions from 1.268g/mL to 1.031 g/mL and collected the fractions containing exosomes. Id1 was barely detected on the surface of exosomes as well as other extracellular vesicles of similar density. However, addition of Triton X-100 (which lyses exosomes) revealed that >80% of the detected Id1 is contained within exosomes, indicating that fibroblasts likely utilize exosomal mechanisms for Id1 export from the nucleus to the cytoplasm and out of the cell.

Id1 is also expressed at high levels in pro-B-cells, but downregulated in pre-B-cells and mature B-cells (25, 26). Constitutive expression of Id1 in transgenic mice shows that these animals display severe defects in the development of B-cells, demonstrating that cells in early development express Id1 and subsequently downregulate it as they acquire a mature phenotype (25). It is tempting to speculate that mature cells in the RA joint may take up fibroblast derived Id1 via exosome release to regulate cell proliferation in the inflammatory milieu of the RA synovium. Cellular crosstalk with Id1 could be a real possibility for transferring information from one cell to another as many inflammatory cells in the RA synovium are unable to make Id1. For example, it was recently reported by Bourdonnay, et al that alveolar macrophages secrete the STAT-induced STAT signaling inhibitors SOCS1 and SOCS3 in exosomes and microparticles, respectively, for uptake by alveolar epithelial cells for subsequent inhibition of STAT activation in vitro and in vivo (27). Kim et al have generated transgenic mice in which Id1 is expressed specifically in T-cells with the total number of thymocytes in these mice being less than 4% of that in Wt mice (28), again demonstrating the repressive nature of Id1 when overexpressed. Most cells were CD4-/CD8- double-negative cells bearing cell surface markers of multipotent progenitor cells, with apoptotic cells constituting about 50% of the total thymocytes. Also of note, Tanaka et al reported that the expression of Id1 in cardiac myocytes leads to the induction of apoptosis through a redox-dependent mechanism (29). Overall, these findings demonstrate that Id1 is present as both a soluble molecule and in EVs that are likely exosome derived from ST fibroblasts.

As previously noted, Id1 is upregulated in RA SF. We show herein that Id1 initiates cell signaling events via a receptor not yet known. We did find that Id1 stimulates EPC signaling through *pP38 and *pJnk at almost all times measured, but not through Erk½ or PI3k. Peak upregulation of *pP38 and *pJnk was found at a stimulation time of ~5 minutes that plateaus at 45 minutes. This is in contrast to HMVECs that display more of a delayed response to Id1, showing significance in *pJnk expression after 15 minutes, then plateauing

at 30 minutes. The kinetics of HMVEC and EPC signaling to Id1 with respect to *pJnk reveals differences in these cells, with the mature EC showing a weaker response to Id1 than EPCs. Nonetheless, this experiment does show that it is possible for *pJnk to be a common signaling molecule in both EPCs and HMVECs when stimulated with Id1. This finding also identifies EPCs and ECs as cells able to bind Id1, further characterizing Id1 as both a vasculogenic and angiogenic mediator in the RA joint (12).

Locating where cell signaling events intersect in mature or progenitor ECs could be used to identify targets for Id1 inhibition and unwanted angiogeneic activity. We have performed similar signaling experiments on RA synovial fibroblasts as shown here for ECs and found that they signal through *pP38, *pJnk, *pJak2 and *pNF-κB in response to Id1 (data not shown), and provides further evidence that Id1 may induce similar signaling events/pathways in various cell types. Of special note is the data (presented in Figure 6) showing that inhibition of Jnk in HMVECs with siRNA significantly reduces the amount of Id1 induced Hb in the mouse Matrigel plug angiogenesis assay. Hb is a direct measure of angiogenesis and we show that Jnk inhibition significantly reduced Id1 driven blood vessel formation in vivo. This finding demonstrates the feasibility of using signaling inhibition to disrupt essential proinflammatory functions (e.g. angiogenesis) initiated by Id1.

In conclusion, we show that Id1 is a pleiotropic nuclear protein exhibiting multiple functions including roles in vasculogenesis, cell growth and cellular self-renewal. We show that Id1 is released from fibroblasts and initiates cell activation, angiogenic and pro-inflammatory properties. We identify Id1 as a fibroblast derived inflammatory protein capable of functioning as a signaling agonist, regulatory molecule and angiogenic mediator in RA tissues.

Author's contributions

GE, CMH, and TI performed the signaling studies. GE, RAO, and CMH performed the staining studies. GE, CMH, SCF performed the ELISA analysis. CMH, WAS, JHR, and PLC performed the *in vivo* Matrigel studies. JHR and MAA performed the K/BxN *in vivo* studies. ASA provided EPCs and assisted in the design of experiments using EPCs. RM isolated the exosomes used in this study. GHK performed pathological analysis on both human and murine tissue sections. DAF assisted with the design of the study and editing of the manuscript. JHR conceived and designed all aspects of the study and drafted the final manuscript. All authors read and approved the final manuscript. All authors have nothing to disclose.

References

1. Gao D, Nolan DJ, Mellick AS, Bambino K, McDonnell K, Mittal V. Endothelial progenitor cells control the angiogenic switch in mouse lung metastasis. Science. 2008;319(5860):195-8.
2. Ward SM, Fernando SJ, Hou TY, Duffield GE. The transcriptional repressor ID2 can interact with the canonical clock components CLOCK and BMAL1 and mediate inhibitory effects on mPer1 expression. The Journal of biological chemistry. 2010;285(50):38987-9000.
3. Swarbrick A, Akerfeldt MC, Lee CS, Sergio CM, Caldon CE, Hunter LJ, et al. Regulation of cyclin expression and cell cycle progression in breast epithelial cells by the helix-loop-helix protein Id1. Oncogene. 2005;24(3):381-9.
4. Kim HJ, Chung H, Yoo YG, Kim H, Lee JY, Lee MO, et al. Inhibitor of DNA binding 1 activates vascular endothelial growth factor through enhancing the stability and activity of hypoxia-inducible factor-1alpha. Molecular cancer research : MCR. 2007;5(4):321-9.
5. Benezra R, Davis RL, Lockshon D, Turner DL, Weintraub H. The protein Id: a negative regulator of helix-loop-helix DNA binding proteins. Cell. 1990;61(1):49-59.
6. Jen Y, Weintraub H, Benezra R. Overexpression of Id protein inhibits the muscle differentiation program: in vivo association of Id with E2A proteins. Genes Dev. 1992;6(8):1466-79.
7. Hara E, Yamaguchi T, Nojima H, Ide T, Campisi J, Okayama H, et al. Id-related genes encoding helix-loop-helix proteins are required for G1 progression and are repressed in senescent human fibroblasts. The Journal of biological chemistry. 1994;269(3):2139-45.
8. Nehlin JO, Hara E, Kuo WL, Collins C, Campisi J. Genomic organization, sequence, and chromosomal localization of the human helix-loop-helix Id1 gene. Biochem Biophys Res Commun. 1997;231(3):628-34.

9. Deed RW, Jasiok M, Norton JD. Nucleotide sequence of the cDNA encoding human helix-loop-helix Id-1 protein: identification of functionally conserved residues common to Id proteins. Biochim Biophys Acta. 1994;1219(1):160-2.
10. Hong SH, Lee JH, Lee JB, Ji J, Bhatia M. ID1 and ID3 represent conserved negative regulators of human embryonic and induced pluripotent stem cell hematopoiesis. Journal of cell science. 2011;124(Pt 9):1445-52.
11. Mellick AS, Plummer PN, Nolan DJ, Gao D, Bambino K, Hahn M, et al. Using the transcription factor inhibitor of DNA binding 1 to selectively target endothelial progenitor cells offers novel strategies to inhibit tumor angiogenesis and growth. Cancer Res. 2010;70(18):7273-82.
12. Isozaki T, Amin MA, Arbab AS, Koch AE, Ha CM, Edhayan G, et al. Inhibitor of DNA binding 1 as a secreted angiogenic transcription factor in rheumatoid arthritis. Arthritis Res Ther. 2014;16(2):R68.
13. Sakurai D, Yamaguchi A, Tsuchiya N, Yamamoto K, Tokunaga K. Expression of ID family genes in the synovia from patients with rheumatoid arthritis. Biochem Biophys Res Commun. 2001;284(2):436-42.
14. Monach P, Hattori K, Huang H, Hyatt E, Morse J, Nguyen L, et al. The K/BxN mouse model of inflammatory arthritis: theory and practice. Methods Mol Med. 2007;136:269-82.
15. Woods JM, Katschke KJ, Volin MV, Ruth JH, Woodruff DC, Amin MA, et al. IL-4 adenoviral gene therapy reduces inflammation, proinflammatory cytokines, vascularization, and bony destruction in rat adjuvant-induced arthritis. Journal of immunology. 2001;166(2):1214-22.
16. Ruth JH, Arendt MD, Amin MA, Ahmed S, Marotte H, Rabquer BJ, et al. Expression and function of CXCL16 in a novel model of gout. Arthritis Rheum. 2010;62(8):2536-44.
17. Sarkar S, Fox DA. Targeting IL-17 and Th17 cells in rheumatoid arthritis. Rheumatic diseases clinics of North America. 2010;36(2):345-66.

18. Park CC, Morel JC, Amin MA, Connors MA, Harlow LA, Koch AE. Evidence of IL-18 as a novel angiogenic mediator. Journal of immunology. 2001;167(3):1644-53.
19. Lyden D, Young AZ, Zagzag D, Yan W, Gerald W, O'Reilly R, et al. Id1 and Id3 are required for neurogenesis, angiogenesis and vascularization of tumour xenografts. Nature. 1999;401(6754):670-7.
20. Maw MK, Fujimoto J, Tamaya T. Role of inhibitor of DNA binding-1 protein is related to angiogenesis in the tumor advancement of uterine endometrial cancers. Exp Ther Med. 2010;1(2):351-6.
21. Volpert OV, Pili R, Sikder HA, Nelius T, Zaichuk T, Morris C, et al. Id1 regulates angiogenesis through transcriptional repression of thrombospondin-1. Cancer Cell. 2002;2(6):473-83.
22. Ciarrocchi A, Jankovic V, Shaked Y, Nolan DJ, Mittal V, Kerbel RS, et al. Id1 restrains p21 expression to control endothelial progenitor cell formation. PLoS ONE. 2007;2(12):e1338.
23. Ohtani N, Zebedee Z, Huot TJ, Stinson JA, Sugimoto M, Ohashi Y, et al. Opposing effects of Ets and Id proteins on p16INK4a expression during cellular senescence. Nature. 2001;409(6823):1067-70.
24. Polsky D, Young AZ, Busam KJ, Alani RM. The transcriptional repressor of p16/Ink4a, Id1, is up-regulated in early melanomas. Cancer Res. 2001;61(16):6008-11.
25. Sun XH. Constitutive expression of the Id1 gene impairs mouse B cell development. Cell. 1994;79(5):893-900.
26. Wilson RB, Kiledjian M, Shen CP, Benezra R, Zwollo P, Dymecki SM, et al. Repression of immunoglobulin enhancers by the helix-loop-helix protein Id: implications for B-lymphoid-cell development. Mol Cell Biol. 1991;11(12):6185-91.

27. Bourdonnay E, Zaslona Z, Penke LR, Speth JM, Schneider DJ, Przybranowski S, et al. Transcellular delivery of vesicular SOCS proteins from macrophages to epithelial cells blunts inflammatory signaling. J Exp Med. 2015.
28. Kim D, Peng XC, Sun XH. Massive apoptosis of thymocytes in T-cell-deficient Id1 transgenic mice. Mol Cell Biol. 1999;19(12):8240-53.
29. Tanaka K, Pracyk JB, Takeda K, Yu ZX, Ferrans VJ, Deshpande SS, et al. Expression of Id1 results in apoptosis of cardiac myocytes through a redox-dependent mechanism. The Journal of biological chemistry. 1998;273(40):25922-8.

Figure 1. *Id1 is expressed on RA STs and K/BxN mouse ankles.* IHC was performed on RA, OA, and NL ST and K/BxN murine cryosections. Tissues were blocked and then incubated using a mouse anti-human Id1 (Abcam) primary antibody (for human tissues) or rabbit anti-mouse Id1 (CalBioreagets) for murine tissues. After washing, tissues were incubated with a biotinylated anti-mouse or anti-rabbit secondary antibody (Vector Labs). Tissues were washed and subsequently developed with the Vectastain ABC kit (Vector Labs). Id1 is found on blood vessels (BV) and on synovial cells (SNC) in the RA ST. Id1 is also found on lining cells near the bone in the K/BxN mouse ankles. This shows the presence of Id1 on pre-fibroblasts/macropage cells as well as cells involved in angiogenesis in both human and mice sections.

Figure 2. *Lining cell (pre-fibroblasts/macropages) Id1 expression is significantly higher in RA ST and can positively correlate with inflammatory score*. A) As shown, Id1 could be seen upregulated on lining cells in RA ST by IHC and significantly correlated with inflammatory score (B). Percentage of cells expressing Id1 were also evaluated on mouse lining cells from joint tissues taken from K/BxN serum induced mice. C) We found mice induced with K/BxN serum had a significantly greater percentage of lining cells expressing Id1 compared to normal (non-induced mice), and that the percentage of Id1 positive lining cells again correlated with the inflammatory score (D). This suggests that lining cell expression of Id1 may be a marker for arthritis severity.

Figure 3. *RA ST fibroblasts make Id1 and can upregulate Id1 expression by stimulation with TGFβ*. Panel A: EPCs, HMVECs, Monocytes, NL, RA, and OA fibroblasts were plated and serum starved. Cell culture media was replaced and the supernatants were collected 24 hours later. The cell culture supernatants were examined for Id1 expression by ELISA (MyBioSource). EPCs were collected from Henry Ford Hospital, HMVECs as well as all

fibroblasts were collected from human tissues which were digested in a mix of cell culture media supplemented with FBS, collagenase, and hyaluronidase. HMVECs were isolated from skin biopsies while the fibroblasts were isolated from STs of patients either RA, OA, or from NL patients. HMVECs were isolated and purified using CD31 microbeads (Miltenyi Biotec). All cell lines were between passages 3 and 6. No cytokine stimulation was used. Panel B: NL fibroblasts were plated and serum starved under the same conditions as Panel A. Cell culture media with the respective cytokine was exchanged and collected 24 hours later. CXCL16 (R&D Systems), IL-17 (R&D Systems), TNF-α (Life Technologies), TGF-β (R&D Systems) was used at 10 ng/mL and 50 ng/mL concentrations. A Not Stimulated (NS) well was also used with no added cytokine (n=no. of experimental replicates). Panel C: Synovial fibroblasts were plated under the same conditions as Panel A. Cell culture media with TGF-β was exchanged and collected 24 hours later. We found that TGF-β has a large effect on Id1 production, and that RA fibroblasts are significantly more sensitive to TGF- β stimulation with respect to Id1 production.

Figure 4. *Id1 is contained within fibroblast exosomes*. Fibroblast culture supernatants were concentrated to 1mL (per flask) by centrifugation through an Amicon Ultracel 30K filter (Millipore). Exosomes were isolated by serial ultracentrifugation. Cells were spun out at 300 x g. Supernatants were cleared of heavier debris by spins at 10,000xg for 30 minutes and 30,000xg for 1 hour. Exosomes were then spun down at 110,000xg for 4-20 hours. Exosome pellets were washed in PBS and spun down again at 110,000 x g. Some exosomes were further purified using a density gradient, Optiprep (Sigma). Id1 was barely detected on the surface of exosomes as well as other EVs of similar density. However, lysing EVs with Triton X-100 (Sigma) revealed that Id1 is contained within exosomes, confirming that Id1 uses exosomal mechanisms for export out of the cell.

Figure 5. *Id1 signals through the *pJnk pathway in HMVECs and EPCs*. HMVECs and EPCs were cultured into 6-well plates and stimulated at different time intervals with human recombinant Id1. The cell lysate was collected and Western blot analysis was performed. The results are shown as fold increase from the non-stimulated (NS), which was arbitrarily set at 1. The upper band represents phosphorylated signaling molecule (*p) and the bottom band represents total signaling molecule. Using these bands, amount of phosphorylated signaling molecule was quantified. Upregulation (↑) of *pJnk and *pP38 was statistically significant in EPCs and upregulation of *pJnk was statistically significant in HMVECs. Upregulation of *pJnk plateaued at 5 minutes in EPCs and later in HMVECs at 30 minutes. Other signaling molecules were tested but results were not significant (data not shown, n=no. of experimental replicates; the delta symbol with slash represents no change (⍙)).

Figure 6. *Jnk siRNA lowers HMVEC mediated angiogenesis in the Matrigel plug assay*. HMVECs were transfected with either control or Jnk siRNA designed to inhibit the Jnk signaling pathway. These cells were combined with 10 nM Id1 in Matrigel, which was injected subcutaneously into mice. 5 days later, the Matrigel plug was removed, weighed, and homogenized. The hemoglobin assay was run to determine amount of hemoglobin in the plugs as a marker of angiogenesis. Jnk siRNA significantly knocked down the amount of angiogenesis in this assay.

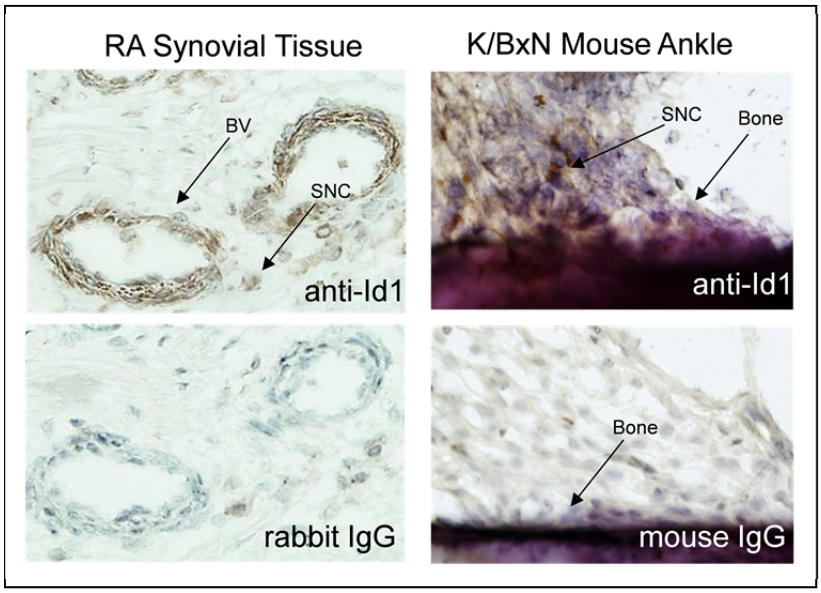

Figure 1. Id1 is expressed on RA STs and K/BxN mouse ankles. IHC was performed on RA, OA, and NL ST and K/BxN murine cryosections. Tissues were blocked and then incubated using a mouse anti-human Id1 (Abcam) primary antibody (for human tissues) or rabbit anti-mouse Id1 (CalBioreagets) for murine tissues. After washing, tissues were incubated with a biotinylated anti-mouse or anti-rabbit secondary antibody (Vector Labs). Tissues were washed and subsequently developed with the Vectastain ABC kit (Vector Labs). Id1 is found on blood vessels (BV) and on synovial cells (SNC) in the RA ST. Id1 is also found on lining cells near the bone in the K/BxN mouse ankles. This shows the presence of Id1 on pre-fibroblasts/macropage cells as well as cells involved in angiogenesis in both human and mice sections.

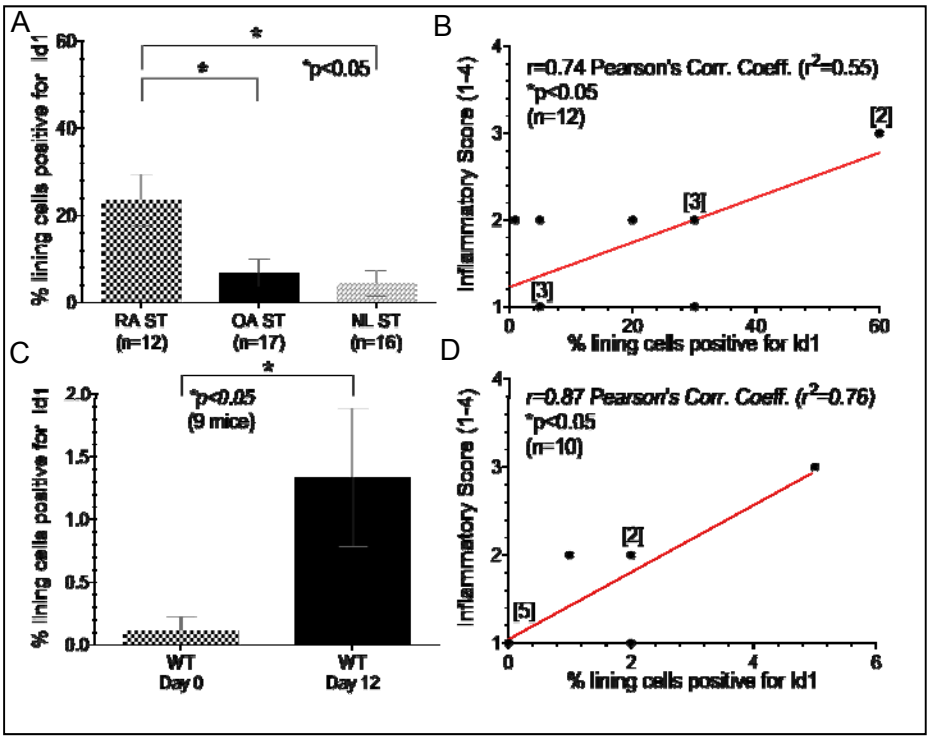

Figure 2. Lining cell (pre-fibroblasts/macropages) Id1 expression is significantly higher in RA ST and can positively correlate with inflammatory score. A) As shown, Id1 could be seen upregulated on lining cells in RA ST by IHC and significantly correlated with inflammatory score (B). Percentage of cells expressing Id1 were also evaluated on mouse lining cells from joint tissues taken from K/BxN serum induced mice. C) We found mice induced with K/BxN serum had a significantly greater percentage of lining cells expressing Id1 compared to normal (non-induced mice), and that the percentage of Id1 positive lining cells again correlated with the inflammatory score (D). This suggests that lining cell expression of Id1 may be a marker for arthritis severity.

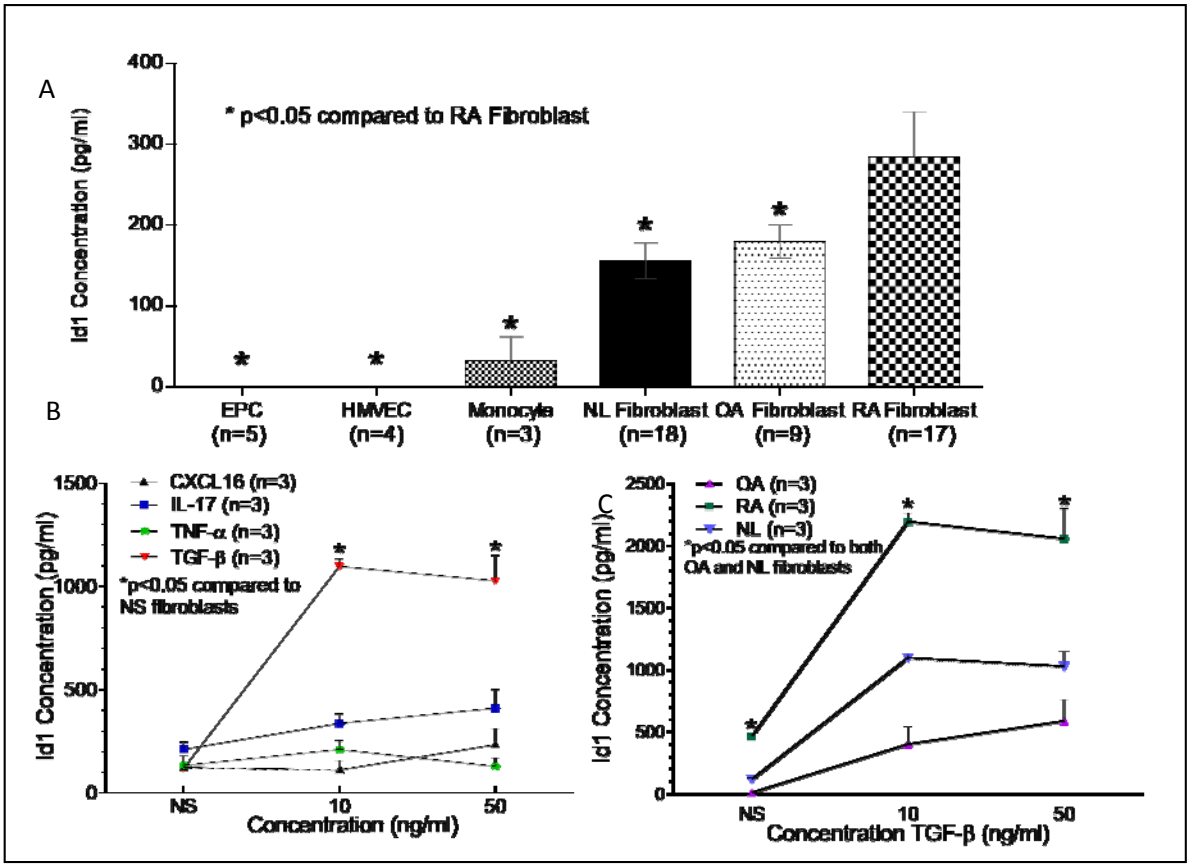

Figure 3. RA ST fibroblasts make Id1 and can upregulate Id1 expression by stimulation with TGFβ. Panel A: EPCs, HMVECs, Monocytes, NL, RA, and OA fibroblasts were plated and serum starved. Cell culture media was replaced and the supernatants were collected 24 hours later. The cell culture supernatants were examined for Id1 expression by ELISA (MyBioSource). EPCs were collected from Henry Ford Hospital, HMVECs as well as all fibroblasts were collected from human tissues which were digested in a mix of cell culture media supplemented with FBS, collagenase, and hyaluronidase. HMVECs were isolated from skin biopsies while the fibroblasts were isolated from STs of patients either RA, OA, or from NL patients. HMVECs were isolated and purified using CD31 microbeads (Miltenyi Biotec). All cell lines were between passages 3 and 6. No cytokine stimulation was used. Panel B: NL fibroblasts were plated and serum starved under the same conditions as Panel A. Cell culture media with the respective cytokine was exchanged and collected 24 hours later. CXCL16 (R&D Systems), IL-17 (R&D Systems), TNF-α (Life Technologies), TGF-β (R&D Systems) was used at 10 ng/mL and 50 ng/mL concentrations. A Not Stimulated (NS) well was also used with no added cytokine (n=no. of experimental replicates). Panel C: Synovial fibroblasts were plated under the same conditions as Panel A. Cell culture media with TGF-β was exchanged and collected 24 hours later. We found that TGF-β has a large effect on Id1 production, and that RA fibroblasts are significantly more sensitive to TGF- β stimulation with respect to Id1 production.

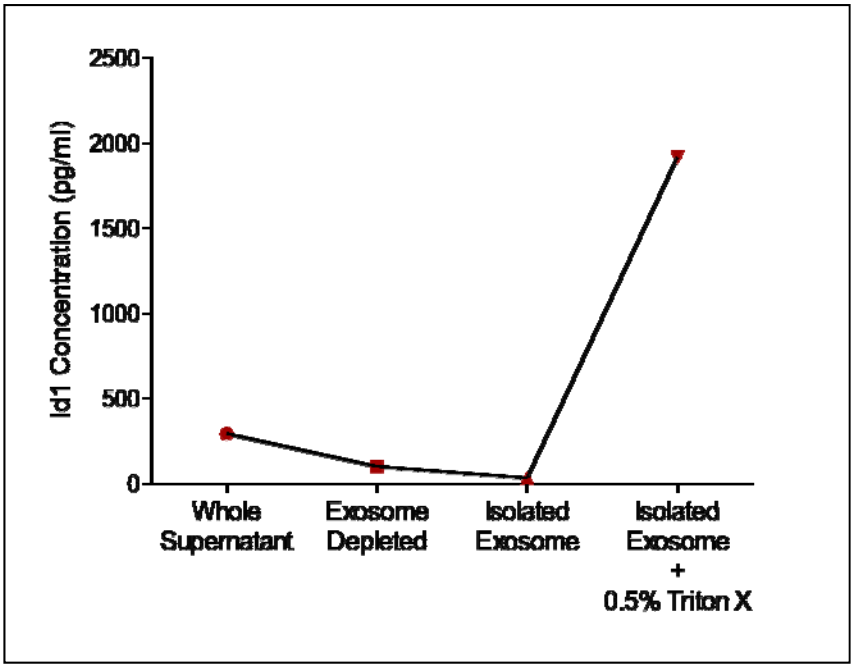

Figure 4. Id1 is contained within fibroblast exosomes. Fibroblast culture supernatants were concentrated to 1mL (per flask) by centrifugation through an Amicon Ultracel 30K filter (Millipore). Exosomes were isolated by serial ultracentrifugation. Cells were spun out at 300 x g. Supernatants were cleared of heavier debris by spins at 10,000xg for 30 minutes and 30,000xg for 1 hour. Exosomes were then spun down at 110,000xg for 4-20 hours. Exosome pellets were washed in PBS and spun down again at 110,000 x g. Some exosomes were further purified using a density gradient, Optiprep (Sigma). Id1 was barely detected on the surface of exosomes as well as other EVs of similar density. However, lysing EVs with Triton X-100 (Sigma) revealed that Id1 is contained within exosomes, confirming that Id1 uses exosomal mechanisms for export out of the cell.

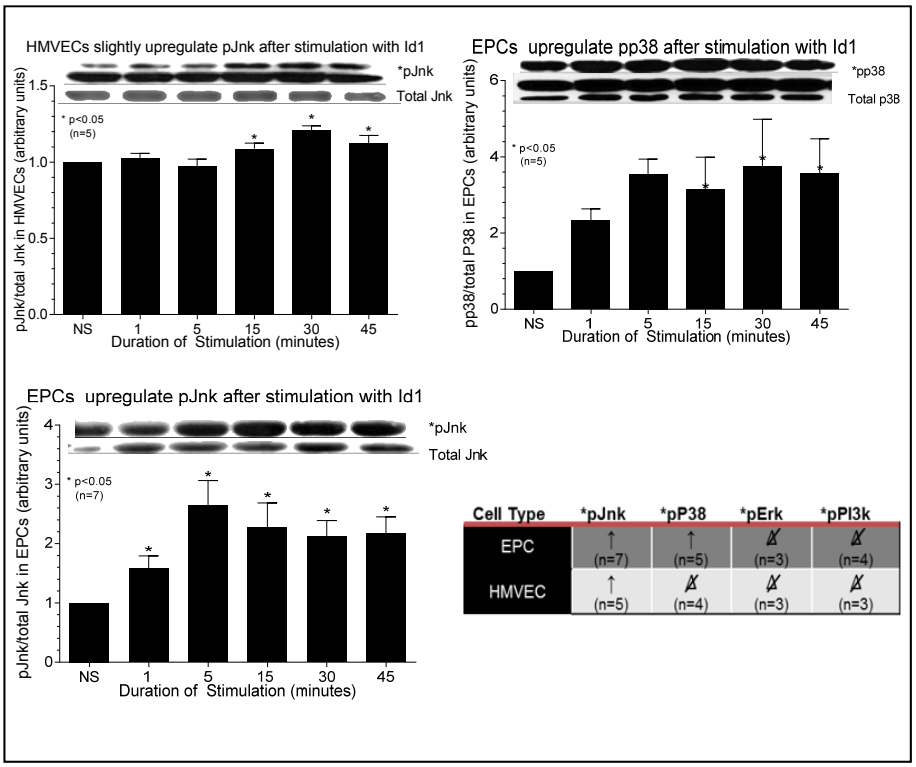

Figure 5. Id1 signals through the *pJnk pathway in HMVECs and EPCs. HMVECs and EPCs were cultured into 6-well plates and stimulated at different time intervals with human recombinant Id1. The cell lysate was collected and Western blot analysis was performed. The results are shown as fold increase from the non-stimulated (NS), which was arbitrarily set at 1. The upper band represents phosphorylated signaling molecule (*p) and the bottom band represents total signaling molecule. Using these bands, amount of phosphorylated signaling molecule was quantified. Upregulation (↑) of *pJnk and *pP38 was statistically significant in EPCs and upregulation of *pJnk was statistically significant in HMVECs. Upregulation of *pJnk plateaued at 5 minutes in EPCs and later in HMVECs at 30 minutes. Other signaling molecules were tested but results were not significant (data not shown, n=no. of experimental replicates; the delta symbol with slash represents no change (Δ)).

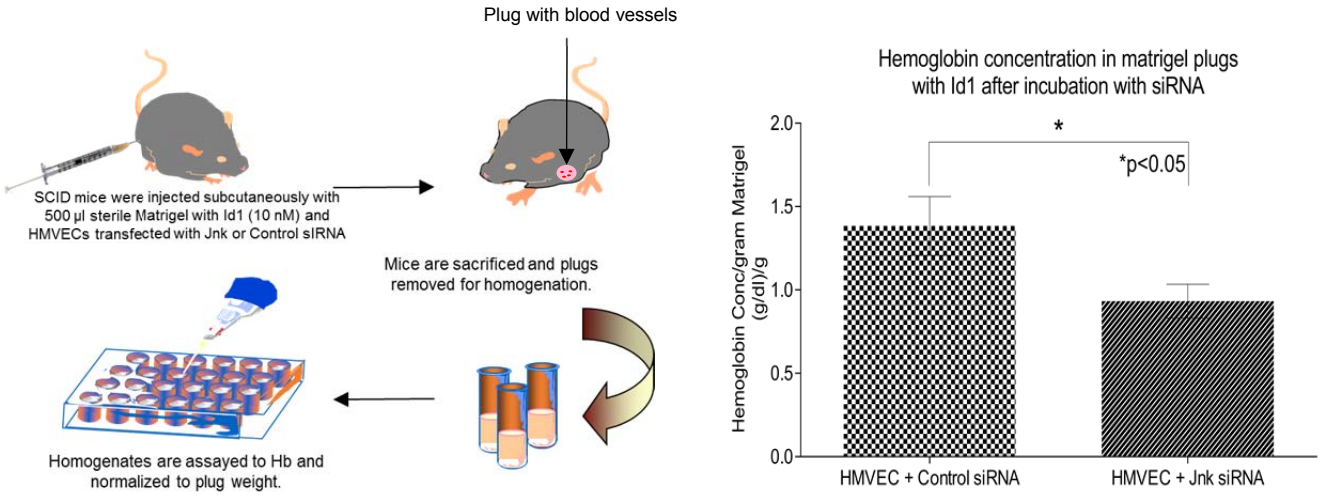

Figure 6. *Jnk siRNA lowers HMVEC mediated angiogenesis in the Matrigel plug assay.* HMVECs were transfected with either control or Jnk siRNA designed to inhibit the Jnk signaling pathway. These cells were combined with 10 nM Id1 in Matrigel, which was injected subcutaneously into mice. 5 days later, the Matrigel plug was removed, weighed, and homogenized. The hemoglobin assay was run to determine amount of hemoglobin in the plugs as a marker of angiogenesis. Jnk siRNA significantly knocked down the amount of angiogenesis in this assay.